ELSEVIER

Journal of South American Earth Sciences 22 (2006) 66–88

Journal of
South American
Earth Sciences

www.elsevier.com/locate/jsames

Structural control on arc volcanism: The Caviahue–Copahue complex, Central to Patagonian Andes transition (38°S)

Daniel Melnick [a,*], Andrés Folguera [b], Victor A. Ramos [b]

[a] *GeoForschungsZentrum Potsdam, Telegrafenberg, D-14473 Potsdam, Germany*
[b] *Laboratorio de Tectónica Andina, Facultad de Ciencias Exactas y Naturales, Universidad de Buenos Aires, CPC1428EHA Buenos Aires, Argentina*

Received 1 March 2004; accepted 1 March 2006

Abstract

This paper describes the volcanostratigraphy, structure, and tectonic implications of an arc volcanic complex in an oblique subduction setting: the Caviahue caldera Copahue volcano (CAC) of the Andean margin. The CAC is located in a first-order morphotectonic transitional zone, between the low and narrow Patagonian and the high and broad Central Andes. The evolution of the CAC started at approximately 4–3 Ma with the opening of the 20×15 km Caviahue pull-apart caldera; Las Mellizas volcano formed inside the caldera and collapsed at approximately 2.6 Ma; and the Copahue volcano evolved in three stages: (1) 1.2–0.7 Ma formed the approximately 1 km thick andesitic edifice, (2) 0.7–0.01 Ma erupted andesitic–dacitic subglacial pillow lavas, and (3) 0.01–0 Ma erupted basaltic–andesites and pyroclastic flows from fissures, aligned cones, and summit craters. Magma ascent has occurred along planes perpendicular to the least principal horizontal stress, whereas hydrothermal activity and hot springs also occur along parallel planes. At a regional scale, Quaternary volcanism concentrates along the NE-trending, 90 km long Callaqui–Copahue–Mandolegüe lineament, the longest of the southern volcanic zone, which is here interpreted as an inherited crustal-scale transfer zone from a Miocene rift basin. At a local scale within the CAC, effusions are controlled by local structures that formed at the intersection of regional fault systems. The Central to Patagonian Andes transition occurs at the Callaqui–Copahue–Mandolegüe lineament, which decouples active deformation from the intra-arc strike-slip Liquiñe-Ofqui fault zone to the south and the backarc Copahue–Antiñir thrust system.

Keywords: Andes; Oblique subduction; Volcanotectonic complex; Arc-parallel faults; Transfer zone

1. Introduction

Subduction-related arc volcanism and magmatism in oblique plate convergence settings are commonly controlled by arc-parallel strike-slip fault zones that accommodate part of the margin-parallel component of oblique subduction (e.g., Fitch, 1972; Beck, 1983; Glazner, 1991; Scheuber and Reutter, 1992; Cembrano et al., 1996; Lavenu and Cembrano, 1999). The degree of strain partitioning along the margin (e.g., Tikoff and Teyssier, 1994) and the internal architecture of these intra-arc fault zones often play important roles in controlling the shape of arc-related volcanic edifices and the orientation of minor eruptive centers (e.g., Nakamura, 1977; Bahar and Girod, 1983; Cashman et al., 1992; López-Escobar et al., 1995; Sieh and Natawidjaja, 2000; Pasquarè and Tibaldi, 2003). We present a case for strong structural control on Plio–Quaternary arc volcanism in an oblique subduction tectonic setting: the Caviahue caldera Copahue volcano complex (CAC) of the Andean convergent margin (Fig. 1) (37°50′S, 71°10′W).

The Andean margin is formed by the subduction of the Nazca plate under the South American plate, at a convergence rate of approximately 80 mm/yr during the past 3 Myr (Somoza, 1998) (Fig. 1). The CAC is composed of the Caviahue caldera and Copahue stratovolcano

* Corresponding author. Fax: +49 331 2881370.
E-mail address: melnick@gfz-potsdam.de (D. Melnick).

0895-9811/$ - see front matter © 2006 Elsevier Ltd. All rights reserved.
doi:10.1016/j.jsames.2006.08.008

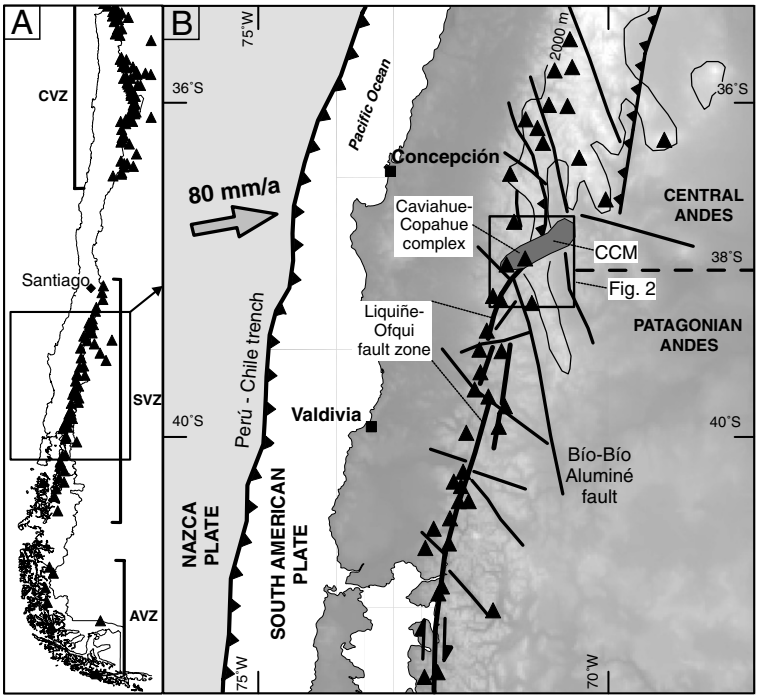

Fig. 1. Location map and main regional structures of the Andean intra-arc zone. Black triangles denote Holocene eruptive centers. (A) CVZ, central volcanic zone; SVZ, southern volcanic zone; AVZ, Austral volcanic zone. (B) CAC, Caviahue–Copahue complex; CCM, Callaqui–Copahue–Mandolegüe transfer zone. Convergence parameters from Somoza (1998).

(Figs. 2A and 3). In terms of geochemical and petrological signatures, this complex is part of the southern volcanic zone (33°–46°S) (Fig. 1), which is characterized by predominantly basaltic to andesitic Quaternary emissions (Hildreth and Moorbath, 1988), and is located within the central petrographical province of the volcanic zone (37°–41°30′S) (Hickey-Vargas et al., 1989). However, in terms of structure, morphology, and tectonics, the CAC is located within a first-order transitional zone between the high and broad Central Andes (3 km mean elevation, up to 800 km wide) and the narrow and low (1 km mean elevation, 300 km wide) Patagonian Andes (Groeber, 1921). This region has a moderately thick crust of approximately 45 km and lies above a zone with a 30° subduction angle of the Nazca plate (Bohm et al., 2002; Lüth et al., 2003). The CAC is one of the more suitable sites to address the relation between lithospheric-scale structures and the development of the volcanic arc in the southern Andean subduction system.

The CAC records activity since the Pliocene epoch with frequent eruptions in recent times. Historical eruptions of the Copahue volcano have been reported since the eighteenth century. A new eruptive cycle started in July 1992, with explosions continuing in 1993 and eruptions during 1994 and September 1995 (Delpino and Bermúdez, 1995). The most recent eruption took place between July and October 2000 (Global Volcanism Network, 2000a,b; Naranjo and Polanco, 2004), and Copahue is now in a fumarolic stage. Activity concentrates in the Agrio crater, a 125 m diameter depression filled with an acid crater lake (pH 0.3, Varekamp et al., 2001) and molten sulfur floating on its surface.

Previous work done in the CAC (Table 1) initially focused on geothermal exploration in Argentina (Dellapé and Pando, 1975; Pesce, 1989; JICA, 1992). Assessment of post-glacial activity and hazards was carried out first in Argentina (Delpino and Bermúdez, 1993, 1995; Martini et al., 1997) and later in Chile (Polanco et al., 2000; Cecioni et al., 2000). Study of the Pliocene pyroclastic deposits (Mazzoni and Licitra, 2000) and a basic stratigraphy based on K–Ar dating took place only in Argentina (Table 1; Pesce, 1989; Delpino and Bermúdez, 1993; Linares et al., 1999). Structural control and regional tectonic implications also have been described in Argentina (Folguera and Ramos, 2000).

We present a structural, volcanostratigraphic, and geomorphological approach based on 1:50,000 scale mapping. The volcanostratigraphic sequence defined in Argentina is improved and extended to the Chilean part of the CAC (Figs. 4, 5). With the improved volcanostratigraphic sequence, we constrain the temporal evolution of the structural systems of the CAC and relate their kinematics to regional features (Folguera, 2002; Melnick, 2004). On the basis of our regional field work, remote sensing data, a digital elevation model, geologic maps (Niemeyer and Muñoz, 1983; Delpino and Deza, 1995; Suárez and Emparán, 1997; SERNAGEOMIN, 2002), and published regional fault kinematic and structural data (Lavenu and Cembrano, 1999; Potent and Reuther, 2001; Melnick et al., 2002; Potent, 2003; Rosenau, 2004), we propose a tectonic control on the opening of the Caviahue caldera.

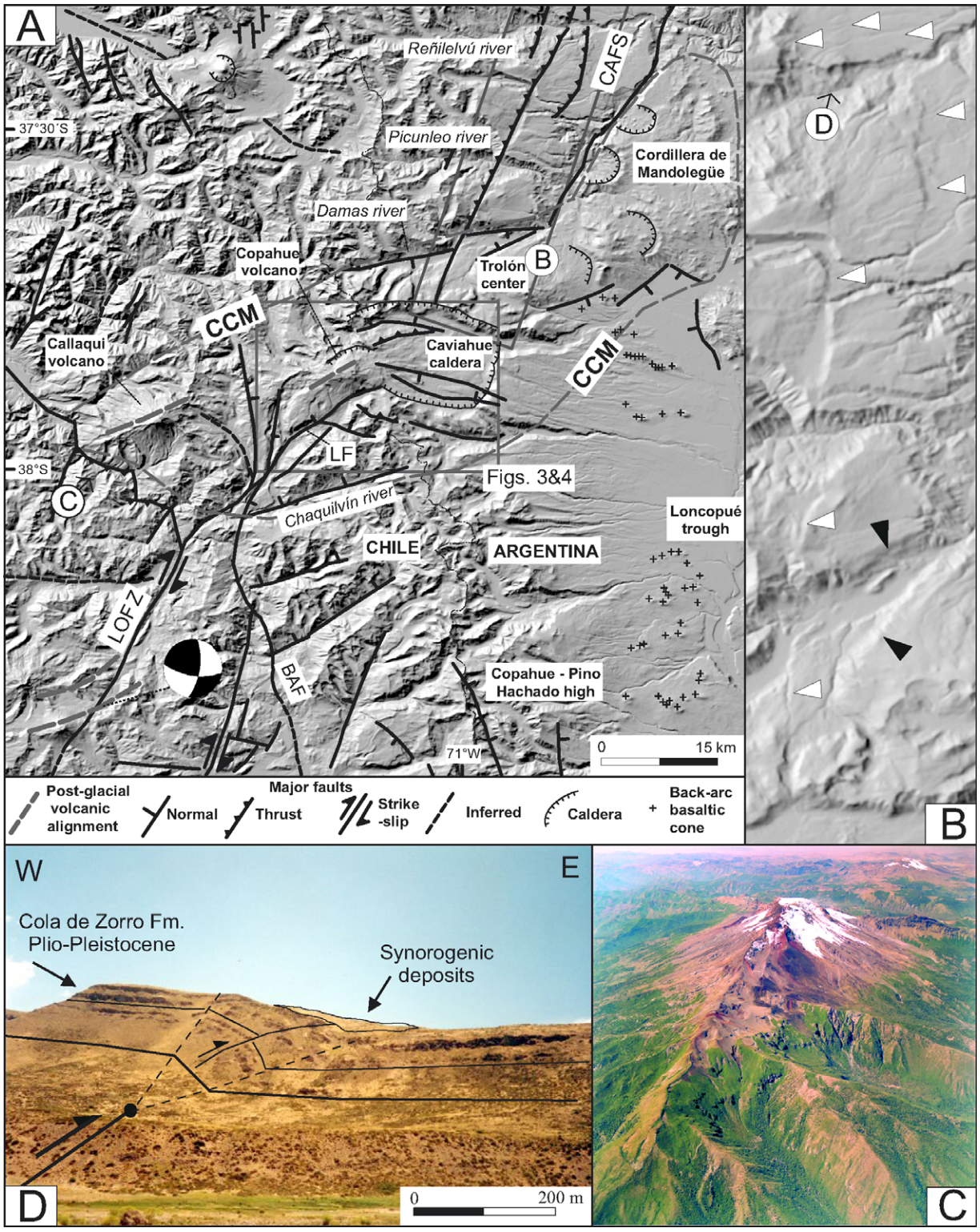

Fig. 2. Regional tectonic features of the Callaqui–Copahue–Mandolegüe (CCM) transfer zone. (A) Shaded-relief digital elevation model from SRTM-Nasa data and structural map. LOFZ, Liquiñe-Ofqui fault zone; BAF, Bío-Bío–Aluminé fault; LF, Lomín fault; CAFS, Copahue–Antiñir fault system. Faults modified from Melnick et al. (2002, 2006) and SERNAGEOMIN (2002). Focal mechanism from Barrientos and Acevedo (1992). (B) Shaded elevation model showing the geomorphology of the Copahue–Antiñir fault system. White triangles show thrust fault scarps, black triangles show normal fault scarps from the Damas half-graben. See (A) for location. (C) Oblique aerial photo to the northeast, along-strike of the CCM. Tension gash morphology of the elongated Callaqui volcano can be observed. The darker flows are post-glacial; below the glacial, a fissure appears. Note the axial valley on the ridge where small craters and fissures are aligned. The snow-covered hill in the back is the Copahue volcano. For location, see (A). (D) View to the north of a monocline cut by a thrust fault at Reñilelvú River. For location, see (B).

2. Geological setting

The CAC is located at the transition between the Central and Patagonian Andes (38°S). The Patagonian Andes are characterized by the absence of a Plio–Quaternary foreland fold-and-thrust belt, unlike the Central Andes. Quaternary deformation in the Patagonian Andes is localized in the intra-arc zone along the arc-parallel strike-slip Liquiñe-Ofqui fault zone (LOFZ), whereas Quaternary shortening is present almost continuously along the Central Andes's eastern foothills (e.g., Dewey and Lamb, 1992). The CAC is located approximately 30 km east of the late Pleistocene–Holocene N–S to NNE-trending volcanic arc (Fig. 1). A previous volcanic front developed between 37°30′ and 39°30′S at the present-day position of the CAC during Pliocene and early Pleistocene times (Muñoz and Stern, 1988).

2.1. The Liquiñe-Ofqui fault zone

The LOFZ is an approximately 1200 km long, intra-arc, dextral strike-slip system that accommodates part of the margin-parallel component of oblique subduction and that has been decoupling a forearc sliver since at least Pliocene times (Figs. 1, 2) (e.g., Hervé, 1976; Hervé, 1994; Nelson et al., 1994; Cembrano et al., 1996, 2000, 2002; Lavenu and Cembrano, 1999; Rosenau, 2004; Rosenau et al., 2006). The LOFZ shows contrasting deformation styles and kinematics along-strike. The southern segment (47°30′–42°S) has been described as transpressive (Lavenu and Cembrano, 1999), controlled by the collision of the Chile Rise (Cembrano et al., 2002). The central segment (42–39°S) is characterized by predominantly strike-slip deformation (Lavenu and Cembrano, 1999; Cembrano et al., 2000; Rosenau, 2004). The northern segment (39–37°50′S), however, shows transtensional deformation, characterized by fault splays, graben formation, and a negative horsetail-like structure (Melnick, 2000; Folguera et al., 2001; Melnick and Folguera, 2001; Potent and Reuther, 2001; Potent, 2003; Rosenau, 2004; Rosenau et al., 2006).

Several studies show that the Quaternary southern volcanic zone is strongly controlled by the LOFZ south of 38°S (e.g., Hervé, 1994; López-Escobar et al., 1995; Lavenu and Cembrano, 1999; Rosenau, 2004). Most stratovolcanoes are either directly emplaced over the main trace of the LOFZ or along arc-parallel and arc-oblique secondary structures (Fig. 1). The morphology of these stratovolcanoes is generally elongated in the NE or NW direction; many have flank or summit fissures and are generally polygenic with several associated groups of aligned parasite cones (e.g., Nakamura, 1977; López-Escobar et al., 1995). Several minor eruptive centers are associated with the LOFZ; most are spatially related to a major center or stratovolcano, but others are formed by isolated clusters of Holocene pyroclastic cones that generally are directly emplaced over the main trace of the LOFZ.

At 38°S, immediately south of the Copahue area, the N–S to NNE-striking LOFZ bends eastward and decomposes into a series of NNW- to NE-striking extensional and transtensional fault splays that form an arrangement with a horsetail-like geometry (Fig. 2A). The NE-striking Lomín fault, further described subsequently, is the main structure of this array.

2.2. The Callaqui–Copahue–Mandolegüe volcanic alignment

The CAC is located in the central sector of the NE-trending, 90 km long Callaqui–Copahue–Mandolegüe (CCM) volcanic alignment, which is the longest Plio–Quaternary alignment of the southern volcanic zone (Fig. 1). From southwest to northeast, the CCM consists of (Fig. 2A):

(1) The active Callaqui volcano, a 3080 m high Quaternary stratovolcano elongated in a N60°E direction (Moreno and Lahsen, 1986). Post-glacial eruption concentrates along an approximately 700 m long fissure near the summit (Fig. 2C) formed by 22 connected individual vents, aligned elongated summit craters, and pyroclastic cones on the northeastern sector. This center has an almost perfect tension gash morphology, 15 km long and 8 km maximum width, as can be seen in the digital elevation model (Fig. 2A) and oblique aerial photo (Fig. 2C).

Table 1
Stratigraphic chart showing the previous volcanostratigraphy proposed for the Caviahue–Copahue complex. Numbers indicate ages in Ma

Age		Pesce (1989)	Delpino and Bermúdez (1993)	Linares et al. (1999)	This paper (Based on ages from Linares et al. (1999))
Ma	Holocene	Copahue volcano	Copahue IV		Copahue volcano (CV) post-glacial stage
0.015	Late Pleistocene	Copahue volcano	Copahue III	Trolón Vn	CV syn-glacial stage 0.7–0.015
				Bayo dome	Cerro Bayo dome 0.6
				Acido dome	CV pre-glacial stage 1–0.7
1.0				Copahue Vn	P.Mahuida dome 1.0
	Early Pleistocene	Trolope avas	Copahue II	Derrames de Fondo Valle	CV pre-glacial stage 1.2–1
		Mellizas Vn			Trolope Lavas 1.4–0.8
1.8	Late Pliocene	Hualcupén Formation	Copahue I	Tobas Pum	Riscos Bayos Ignimbrite 2.0
3.4	Early Pliocene			Las Mellizas	Las Mellizas Sequence 2.6
				Hualcupén Formation	Cola de Zorro Formation 5.6–4.0
5.2					

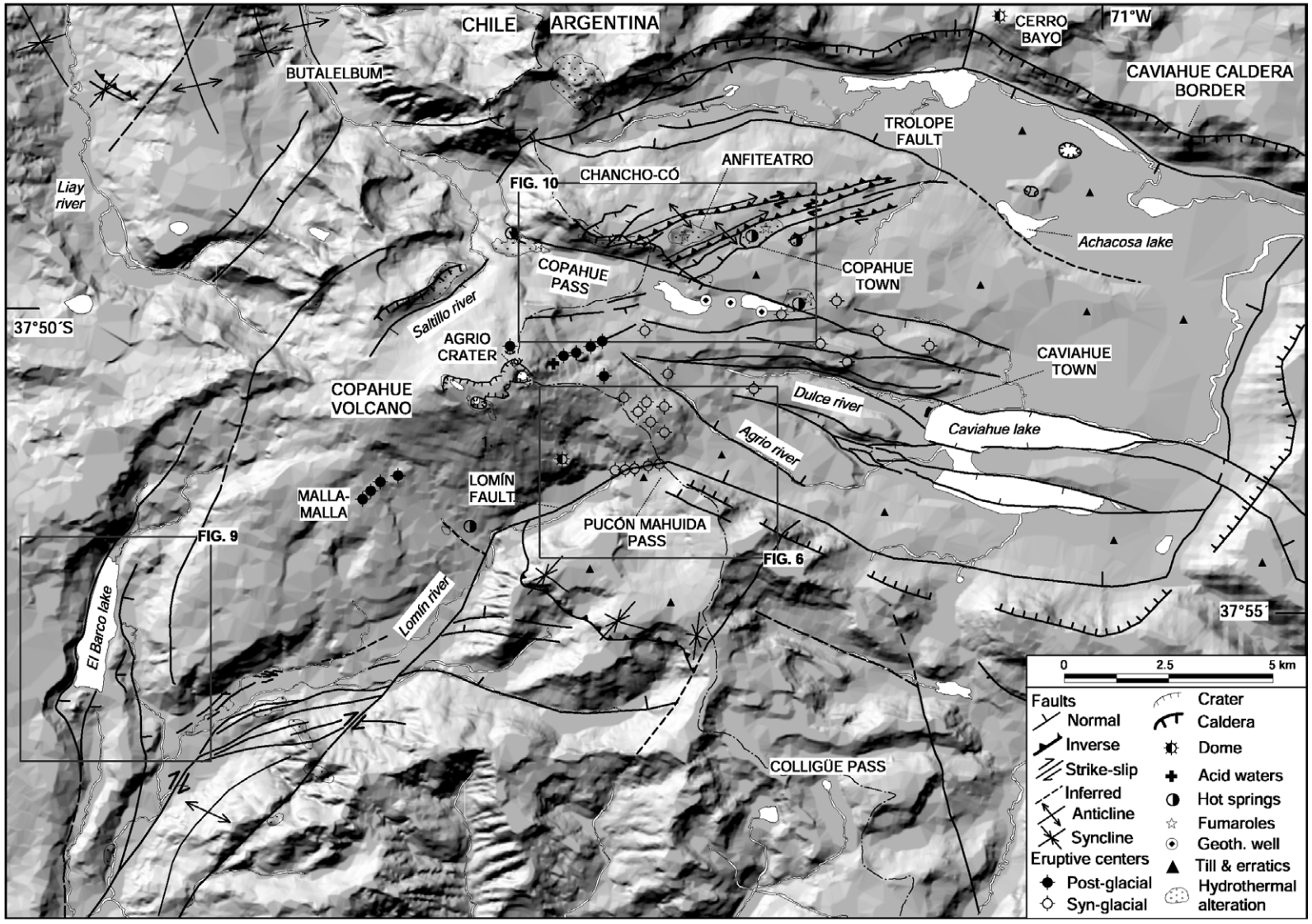

Fig. 3. Shaded-relief digital elevation model based on 1:50,000 topomaps merged with SRTM data east of 71°W. Drainage network and structures of the Caviahue–Copahue complex. Local names referred in the text; locations of Figs. 3, 6, and 10 shown.

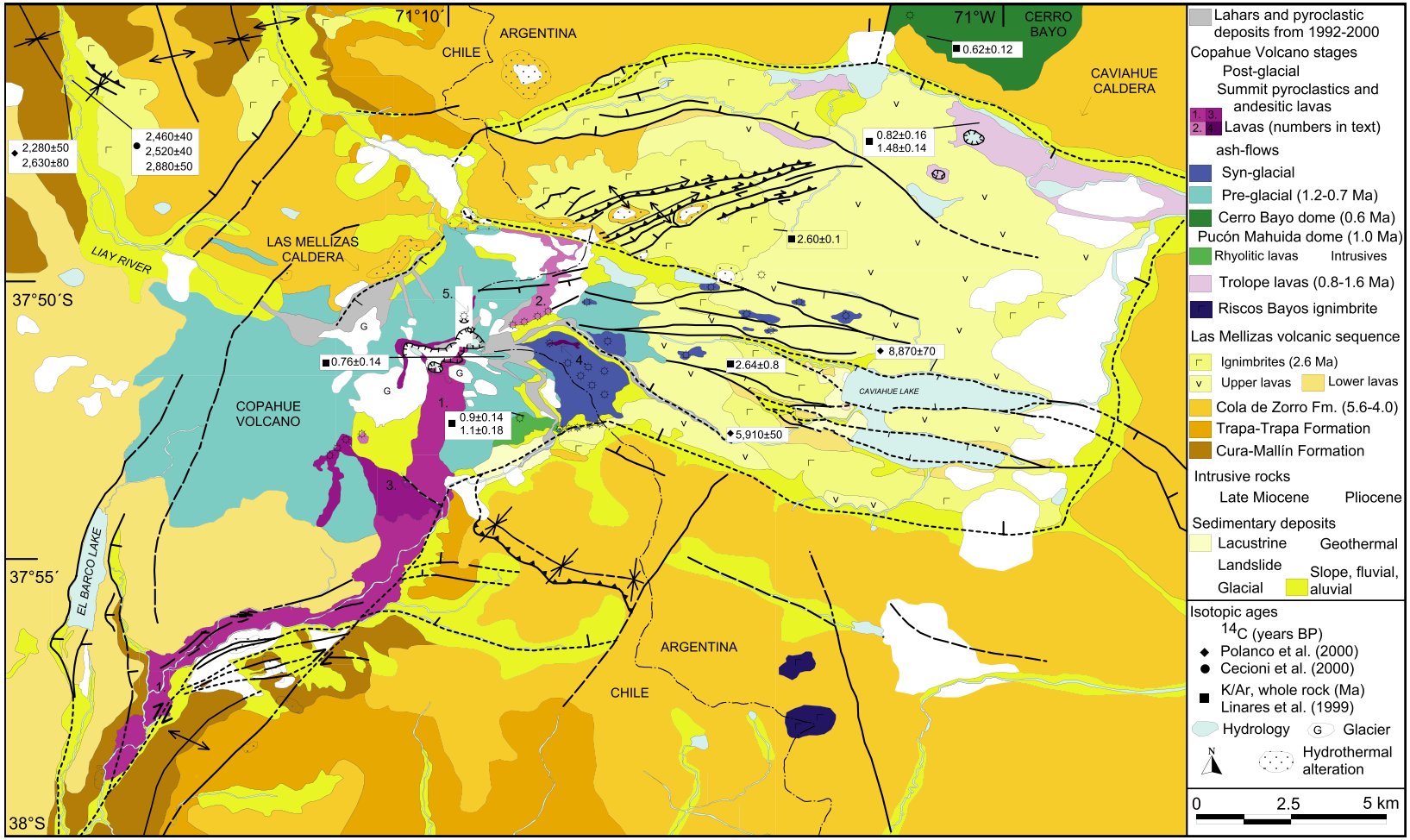

Fig. 4. Geology of the Caviahue caldera Copahue volcano complex based on 1:50,000 scale mapping. Short stippled lines indicate covered faults.

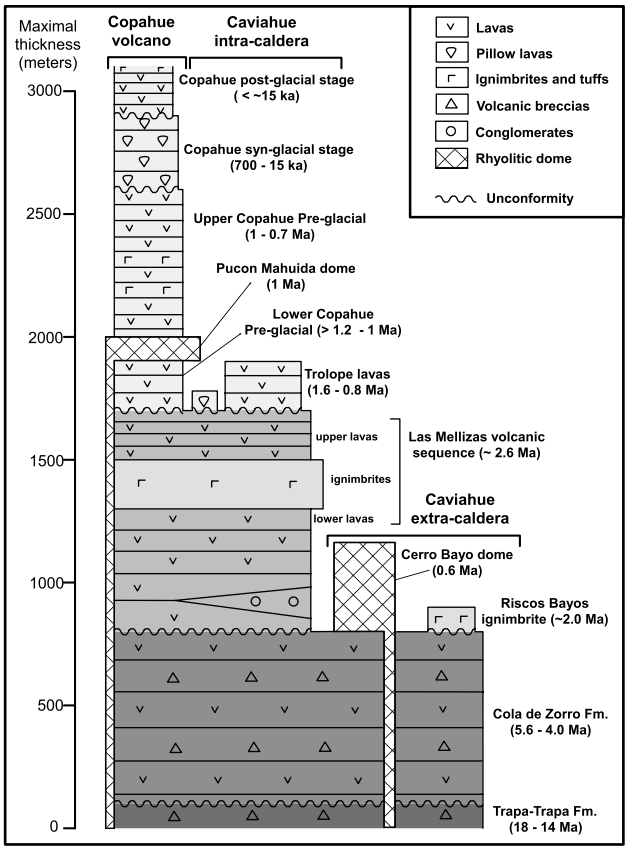

Fig. 5. Generalized stratigraphic chart of the Caviahue–Copahue complex, showing the main lithologies and maximal thicknesses of the units.

(2) The CAC, formed by the Caviahue caldera and Copahue stratovolcano, on which this article focuses.
(3) The Trolón volcanic center, a small, partially collapsed, andesitic stratovolcano with a K–Ar age at the base of 0.6 ± 0.14 Ma (Linares et al., 1999) and three post-glacial vents aligned in a NE direction.
(4) The Cordillera de Mandolegüe, a 40 km long, fault-bounded elongated block composed of partially collapsed Quaternary stratovolcanoes, small caldera rims, NE-trending dyke swarms, and pyroclastic cones elongated in the same direction (Fig. 2A).

Carpinelli (2000) and Radic et al. (2002), on the basis of regional stratigraphic and structural data and basin modeling, infer that between 37° and 39°S, the Cura-Mallín Basin was an intra-arc rift depocenter formed by two diachronic subbasins. Both subbasins had a hemigraben geometry and were limited by a ENE-oriented transfer zone located at approximately 38°S. Their data show that this transfer zone was active during an Oligocene–middle Miocene extensional stage of the basin and also during the late Miocene inversion phase. We propose, following the arguments in Melnick et al. (2002), that the CCM is the Plio–Quaternary expression of the transfer zone postulated by Carpinelli (2000) and Radic et al. (2002) for the Cura-Mallín Basin and therefore a crustal-scale structure.

South of the CCM, an uplifted block representing the Pliocene–early Pleistocene volcanic arc extends to 39°30′S. This block, the Copahue–Pino Hachado high (Muñoz and Stern, 1988), is limited to the east by the Loncopué trough, a Quaternary tectonic depression (Ramos, 1977) filled with backarc monogenetic alkaline basalts (Muñoz and Stern, 1989), and to the west by the Bío-Bío–Aluminé fault (Muñoz and Stern, 1988) (Fig. 2A).

2.3. The Copahue–Antiñir thrust system

North of the CCM, the Copahue–Antiñir thrust system develops in the backarc along the Argentinean foothills (Ramos and Folguera, 1999; Melnick et al., 2002; Folguera et al., 2004). This compressive system folds and faults a sequence of volcanic rocks with interbedded fluvial and alluvial conglomerates that have spatial-lateral continuity and are thus correlated with the Plio–Pleistocene Cola de Zorro Formation, defined immediately to the west in Chile (González and Vergara, 1962). Isotopic K–Ar ages for this unit range from 5.6 ± 0.1 to 1.0 ± 0.2 Ma between 36° and 39°S (Vergara and Muñoz, 1982; Niemeyer and Muñoz, 1983; Suárez and Emparán, 1997; Linares et al., 1999; Folguera et al., 2004).

The Copahue–Antiñir system extends from 37°50′S northward for approximately 90 km with a concave to the west trace (Figs. 2A and B); its northern end is not well studied. This system consists of imbricated high-angle reverse faults and folds, which form individual fault scarps up to 150 m high. These structures control the main slope break in the eastern foothills of the Main Cordillera.

The geomorphology and geometry of the southern part of this fold-and-thrust system is illustrated by the shaded relief elevation model in Fig. 2B. In general, the scarps cut a relatively flat relief formed by basaltic plateau lavas. The offset of ephemeral landforms, mainly gullies, crests, and rivers, indicates minor dextral transpressional deformation in the southern part of the system at around 37°35′–37°25′S (Fig. 2B). Sag ponds are present close to the fault scarps in the footwalls, and small perched streams occur on the hangingwalls. At Reñilelvú River (Fig. 2A), an east-facing monocline is cut by an east-vergent thrust fault, and colluvial syntectonic deposits accumulate in the face of the monocline (Fig. 2C). Also in this area, at a road cut along the international road to Pichachén pass, semiconsolidated, fluvial conglomerates and pyroclastic beds from the base of the Cola de Zorro Formation are folded and exposed in a vertical position, unconformably covered by colluvial syntectonic deposits. Approximately 25 km south, at Picunleo River (Fig. 2A), high-angle reverse faults and east-vergent fault propagation folds affect late Pleistocene glaciolacustrine deposits (Iaffa et al., 2002). Hermanns et al. (2003) note that a cluster of post-glacial rock avalanches is in close spatial association with the trace of this fault system and relate them to slope instability triggered by paleoearthquakes. The

occurrence of fresh surface ruptures and many late Quaternary backarc pyroclastic cones emplaced along the trace of this fault system lead Folguera et al. (2004) to propose that the system is currently active, despite the lack of substantial crustal seismicity.

3. Volcanostratigraphy of the Caviahue caldera-Copahue volcano complex

The following volcanostratigraphic sequence is based on relations observed in the field, available isotopic ages, and a preliminary sequence proposed by Linares et al. (1999) in Argentina (Tables 1 and 2). Herein, we improve the sequence and extend it to Chile to cover the CAC completely (Figs. 3–5).

3.1. Cola de Zorro formation

This unit was originally defined in Chile by González and Vergara (1962) as a sequence of subhorizontal basaltic to andesitic lavas, volcanic breccias, and minor sedimentary beds continuously exposed in the Main Cordillera between 36 and 39°S. The Cola de Zorro Formation was deposited prior to the opening of the Caviahue caldera and forms its basement and walls. K–Ar ages of this unit range from around 5 to 1 Ma between 36° and 39°S (Vergara and Muñoz, 1982; Niemeyer and Muñoz, 1983; Suárez and Emparán, 1997; Linares et al., 1999). This unit overlies all Oligo–Miocene sequences in a marked angular unconformity. Regional observations of abrupt changes of thickness from 100 to 1200 m, normal faulting, and related block tilting within the sequence lead Folguera et al. (2003) to propose an extensional tectonic regime during the deposition of this unit. Eight K–Ar ages from samples taken in the inner wall of the Caviahue caldera area (Table 2) indicate that the Cola de Zorro Formation was deposited between 5.6 ± 0.1 and 4.0 ± 0.1 Ma (Muñoz and Stern, 1988; Linares et al., 1999). This unit is equivalent to the locally defined Hualcupén Formation (Pesce, 1989), but we prefer to use Cola de Zorro Formation because it is a regionally defined unit.

Table 2
Compiled K/Ar ages from the Caviahue–Copahue complex

Sample No.	Lithology/method	% K	^{40}Ar rad (nl/g)	% Ar (atm)	Age and error (2σ)	Reference
Cola de Zorro Formation (inner wall of the Agrio caldera)						
CO-2	BA/WR	1.03	0.076	80.3	4.25 ± 0.10	Linares et al. (1999)
CO-10	BA/WR	1.41	0.098	58.2	4.00 ± 0.10	Linares et al. (1999)
CO-23	AN/WR	1.19	0.105	69.9	5.08 ± 0.14	Linares et al. (1999)
CO-32	BA/WR	1.27	0.105	73.1	5.67 ± 0.14	Linares et al. (1999)
CO-47	BA/WR	1.80	0.133	92.0	4.26 ± 0.10	Linares et al. (1999)
CO-48	BA/WR	1.65	0.119	71.3	4.15 ± 0.10	Linares et al. (1999)
AG-1	AN/WR	1.18	0.102	52.8	4.98 ± 0.14	Linares et al. (1999)
TC-38	AN/WR	1.27	0.215	84	4.3 ± 0.6	Muñoz and Stern (1988)
Las Mellizas volcanic sequence						
CO-22	AN/WR	1.70	0.078	62.2	2.64 ± 0.08	Linares et al. (1999)
CO-33	AN/WR	1.82	0.082	42.4	2.60 ± 0.10	Linares et al. (1999)
CO-34	BA/WR	2.58	0.120	77.4	2.68 ± 0.14	Linares et al. (1999)
Riscos Bayos ignimbrite						
CO-1	RI/WR	3.51	0.127	77.8	2.08 ± 0.16	Linares et al. (1999)
CO-3	RI/BIO	6.76	0.241	90.6	2.05 ± 0.10	Linares et al. (1999)
TC-38	RI/BIO	6.78	0.296	94	1.1 ± 0.5	Muñoz and Stern (1988)
Copahue volcano						
CO-36	AN/WR	1.79	0.036	95.5	1.16 ± 0.10	Linares et al. (1999)
CO-37	DA/WR	2.88	0.038	84.0	0.76 ± 0.14	Linares et al. (1999)
CO-3 9	TA/WR	2.34	0.058	27.8	1.23 ± 0.18	Linares et al. (1999)
CO-40	AN/WR	2.35	0.037	75.9	0.91 ± 0.14	Linares et al. (1999)
TC-31	AN/WR	1.86	0.060	82	0.8 ± 0.1	Muñoz and Stern (1988)
Pucón Mahuida dome						
CO-19	RY/WR	3.53	0.055	77.5	0.90 ± 0.14	Linares et al. (1999)
CO-20	RY/WR	3.50	0.067	68.8	1.10 ± 0.18	Linares et al. (1999)
Cerro Bayo dome						
BA-01	RY/WR	3.22	0.034	94.5	0.60 ± 0.12	Linares et al. (1999)
Trolope lava flows						
CO-7	DI/WR	2.51	0.071	83.4	1.63 ± 0.10	Linares et al. (1999)
CO-29	AN/WR	2.65	0.050	79.3	1.09 ± 0.10	Linares et al. (1999)
CO-49	AN/WR	1.67	0.043	88.0	1.48 ± 0.14	Linares et al. (1999)
CO-52	AN/WR	2.61	0.037	93.3	0.82 ± 0.16	Linares et al. (1999)

Lithologies: AN, andesite; BA, basaltic–andesite; DA, dacite; RY, rhyolite; RI, rhyolitic ignimbrite; dacitic ignimbrite; TA, traquiandesite. Methods: WR, whole-rock; BIO, biotite.

3.2. Las Mellizas volcanic sequence

This unit was defined by Pesce (1989) in Argentina; its outcrops are restricted to the interior of the Caviahue caldera and to the western surroundings of the Copahue volcano in Chile (Fig. 4). In regional terms, this volcanic sequence could be correlated with the Cola de Zorro Formation, but on the basis of our field observations, the lithological differences with the Cola de Zorro unit in the area, the ability to define an emission center, and available isotopic ages, we individualize it.

In Liay River, Chancho-Có and Pucón Mahuida pass areas, Las Mellizas sequence overlies the 5° to 10° tilted Cola de Zorro Formation in an erosional unconformity. In the interior of the Caviahue caldera, it is in tectonic contact by normal faults with the Cola de Zorro Formation (Fig. 4). In El Barco Lake area, Las Mellizas sequence overlies the Cura-Mallín Formation in strong angular unconformity. K–Ar ages (Table 2) range from 2.68 ± 0.14 to 2.60 ± 0.1 Ma (Linares et al., 1999), which might indicate it was deposited after an approximate 1.5 Ma hiatus in volcanism or erosional period in the area, though the available ages are not enough to affirm this observation. Las Mellizas sequence fills the Caviahue caldera completely and is not exposed above its borders. Therefore, it is considered as first post-caldera unit.

According to our detailed mapping, Las Mellizas volcanic sequence is subdivided into three lithofacies: lower lavas, ignimbrites, and upper lavas (Figs. 4 and 5). Because correlation among outcrops from distant locations is difficult, local sequences are only tentatively integrated into a representative section (Fig. 5). Local names are shown in Fig. 3.

3.2.1. Lower lavas

This lithofacies crops out only locally in Argentina inside the Caviahue caldera but extensively in the Chilean part of the CAC, where the thicknesses reach 500 m. It underlies the ignimbrites and unconformably overlies the Cura-Mallín Formation. Near the town of Caviahue, this lithofacies is represented by remarkably columnar-jointed lavas of basaltic to andesitic composition. Sedimentary deposits are interbedded in the lavas along the river, west of Caviahue. They have 30 m minimum thickness and are of alluvial or laharic origin, with angular volcanic blocks of up to 70 cm.

3.2.2. Ignimbrites

This andesitic to dacitic lithofacies is widespread inside the Caviahue caldera and around the northern and northwestern areas of the Copahue volcano (Fig. 4). Out-of-place blocks were found west of the volcano. The maximal thickness, measured from field exposures, is 200 m in the central part of the caldera, whereas the minimum is 5 m near the town of Copahue. A vitrophyre is present nearly everywhere at the base with variable thicknesses of 50–3 m. Vertical gradations among eutaxitic texture, pseudo flow-banding, and complete homogenization to glassy texture are commonly observed. Mazzoni and Licitra (2000) note that the ignimbrites have lateral textural variations, from rheomorphic to eutaxitic, and are massive with lithic clasts. Rheomorphic andesitic ignimbrites crop out at Copahue and Chancho-Có, with thicknesses less than 10 m. Ignimbrites with eutaxitic texture typically enclose black glassy fiamme up to 10 cm long. Lithic clast-bearing ignimbrites are exposed on the eastern and northern margins of the caldera, where they reach 170 m thick. The lateral variations in thickness and texture may reflect emplacement on a significant paleorelief, in which thin rheoignimbrites could represent deposition on topographic highs, whereas thick clast-bearing ignimbrites were deposited in a channeled surface or close to steep slopes.

3.2.3. Upper lavas

This lithofacies is the dominant facies filling most of the Caviahue caldera with thicknesses that reach 200 m. It is composed of predominantly andesitic lavas with characteristic sheet-like horizontal fractures and homogenous thicknesses and textures. These lavas overlie the ignimbrites and are covered by flows from the Copahue volcano.

3.2.4. Volcanic setting of Las Mellizas sequence

Pesce (1989) proposes that Las Mellizas sequence represents an eroded stratovolcano, whose emission center would have been located at the Cerro Las Máquinas, where an andesitic volcanic neck is exposed and also where the Copahue volcano is at present. Mazzoni and Licitra (2000) associate the ignimbrites with intracaldera flows and relate them to the collapse of the Caviahue caldera and the Riscos Bayos ignimbrite (described subsequently) as contemporaneous extracaldera flows, though no collapse breccias are exposed inside the caldera. We agree that this unit represents an eroded stratovolcano, in line with Pesce (1989), whose main emission center was where the Copahue volcano is located at present, where remnants of an eroded edifice crowned by a moderate cuspidate caldera are preserved (Las Mellizas caldera, Fig. 4). Only the northern rim of this caldera is preserved at Copahue pass and Saltillo River (Fig. 3) as an approximately 4 km diameter circular scarp with adjacent hydrothermal alteration zones. The walls of this scarp are formed by lavas and breccias of the Cola de Zorro Formation, and the Copahue volcano is emplaced in its center. Las Mellizas caldera seems partly nested in the Caviahue caldera.

We propose that the ignimbrites represent the collapse of Las Mellizas stratovolcano, which caused the cuspidate caldera originally mapped by Pesce (1989). This interpretation is supported by the increase in thickness of the ignimbrites in areas of lower relief away from the source, as well as by the facies distribution. The ignimbrites are not restricted to the interior of the Caviahue caldera, as proposed by Mazzoni and Licitra (2000), who studied only the Argentinean part of the complex; remnants are widespread in

Chile, up to 14 km west and 10 km north of the Caviahue caldera border (Fig. 4). Therefore, we do not relate the ignimbrites to intracaldera flows of the Caviahue caldera as Mazzoni and Licitra (2000) did. In turn, we support the original proposition of Pesce (1989) that invokes the existence of Las Mellizas volcano. The position of this eruptive center is consistent with our mapping of all the lithofacies of Las Mellizas volcano that surround the former emission center and are spatially restricted units.

3.3. Riscos Bayos ignimbrite

This pyroclastic unit was first recognized by Muñoz and Stern (1988) and is exposed mostly in the southeastern outer slope of the Caviahue caldera with a thickness of approximately 250 m, covering an area of around 30 km^2. It is also exposed near Colligüe pass as two isolated bodies covering areas of 0.5 and 1.1 km^2, with thicknesses of approximately 150 m (Fig. 4). In the outer caldera area, this unit is formed by a rhyolitic ignimbrite dated by K–Ar in biotite as 1.1 ± 0.5 Ma (Muñoz and Stern, 1988) and 2.05 ± 0.10 Ma (Linares et al., 1999) (Table 2).

The Riscos Bayos ignimbrite has been related to the collapse of the Caviahue caldera (Muñoz and Stern, 1988; Pesce, 1989; JICA, 1992; Mazzoni and Licitra, 2000), though the reported ages for the first post-caldera unit are older according to our field observations of Las Mellizas volcanic sequence. The ages reported for this unit by Muñoz and Stern (1988) and Linares et al. (1999) differ by about 1 Ma, indicating they were either significantly influenced by analytical errors, contamination, or xenocrists or taken from different deposits and therefore not reliable. Better geochronological work is needed to constrain the age of this unit and its volcanological context.

3.4. Trolope lava flows

This unit, originally described by Pesce (1989), is exposed in the northern part of the caldera as an approximately 200 m thick succession of homogeneous andesitic lava flows and breccias. These lavas extend eastward out of the caldera and cover an area of about 50 km^2. Individual lava flows reach thicknesses of 2–3 m and breccias about 0.5–1 m. Linares et al. (1999) report four K–Ar ages for this unit that range from 1.63 ± 0.1 to 0.82 ± 0.16 Ma (Table 2). The extent of these flows is limited to the northeastern part of the Caviahue caldera, where they are partially covered by glacial deposits. Mostly on the basis of the interpretation of remote sensing images, previous workers have mapped ignimbrites and basaltic lavas as part of the Trolope flows in the northwestern area of the caldera (Pesce, 1989; Linares et al., 1999; Mazzoni and Licitra, 2000; Folguera and Ramos, 2000; Melnick and Folguera, 2001). The detailed mapping of this area during the current field survey enables us to define the exposures of the Trolope flows and group the ignimbrites and basaltic lavas of Las Mellizas sequence on the basis of their lithological and textural similarities and continuous exposures to the south and southwest (Fig. 4).

The Trolope flows are restricted to the northeastern border of the caldera, where they fill a flat depression. Two elliptical craters are associated with these flows; their long axes are 550 and 340 m and their short axes 400 and 250 m, yielding a similar length-to-width ratio of about 1.4 for both craters. The shape of the elliptical craters or cones can indicate the orientation of a feeder fault or dyke oriented parallel to the long axis of the crater, base of the cone, or apical depression of a dome (e.g., Tibaldi, 1995; Pasquarè and Tibaldi, 2003). The long axis of both craters is oriented WNW–ESE, parallel to the northern caldera border normal fault (Fig. 3). The Trolope fault (Figs. 3 and 4) is a WNW-trending, north-down normal fault that bounds the south of the depression filled by the Trolope andesitic flows and locally offsets them by up to 40 m (Fig. 4). This fault is parallel to the northern caldera border normal fault and the long axis of both elliptical craters.

3.5. Copahue volcano sequence

This polygenetic, 3025 m high stratovolcano is located on the western margin of the CAC (Figs. 2–4) and concentrates most recent volcanic activity of the complex. On the basis of our field observations and available isotopic ages, we propose to subdivide the evolution of the Copahue volcano into three main stages. This subdivision relies on the stratigraphic relations observed in the field and textural and structural differences among the volcanic products. The basal andesitic lavas and pyroclastic flows, which evidence glacial erosion and form the volcanic edifice, are grouped in the preglacial stage; andesitic to dacitic lavas that overlie the former stage and exhibit textural and structural characteristics that imply eruptions in contact with ice are grouped in the synglacial stage; and homogeneous basaltic–andesitic lavas and pyroclastic flows that overlie the products of the former stages and have no evidence of glacial erosion are grouped in the post-glacial stage.

3.5.1. Preglacial stage 1

Up to 1000 m thick, this sequence is formed mostly by vitreous lavas and minor pyroclastic flows that form the edifice of the Copahue volcano. These lavas have no significant textural variations, homogeneous thicknesses, and basaltic–andesitic to andesitic composition (52.48–61.1% SiO_2, Cecioni et al., 2000). Isotopic ages indicate that the Copahue edifice was built during lower Pleistocene times, between 1.23 ± 0.18 and 0.76 ± 0.14 Ma (Muñoz and Stern, 1988; Linares et al., 1999). The youngest sample dated by Linares et al. (1999) was taken near the eastern part of the summit (Fig. 4), confirming that the edifice was built during early Pleistocene time. The basal lavas of this stage, exposed on the southeastern flank (Fig. 3), are intruded by the Pucón Mahuida dome, but the upper part of these lavas clearly overlies the dome. The isotopic ages are consistent with these field observations (Table 2).

3.5.2. Synglacial stage 2

In contrast with the previous episode during which the Copahue edifice was built, this stage is characterized by the emission of relatively minor volumes of lava from aligned vents. Emissions concentrate in a flat-topped, rounded lava mountain located on the southeastern flank of the volcano. This body has the geometry of a dome, extending more than 5.5 km^2 with 300 m average thickness (Figs. 3 and 6A). The lavas range in composition from andesitic to dacitic (58.2–63.6% SiO_2, Cecioni et al., 2000), and have typical features of magma–water interaction in the sense of Lescinsky and Fink (2000), such as polygonal and hackly fractures, glassy margins with pseudopillow cracks, and well-developed pillow-lava structures (Fig. 6D). Several lava tubes were formed over the flat-topped mountain (Fig. 6C). Subglacial or tardiglacial melting-related eruptions might be suitable scenarios for these features.

These lavas overlie all the products from the former stage 1 whose youngest K–Ar age is 0.76 ± 0.14 Ma, constraining this synglacial stage to one or more of the glacial periods of the past 700 ka. The lava tubes and isolated pillow lava vents observed on top of the dome-like body are well preserved and show no evidence of glacial erosion (see aerial photo in Fig. 6B), in contrast with the Pliocene–lower Pleistocene units, whose surface has marks of glacial abrasion and is covered by till deposits and small erratic blocks. This difference implies that at least the upper part of the dome-like body formed during the last glacial period, well constrained in the Patagonian Andes between 75 and 15 ka (e.g., Lowell et al., 1995).

At Pucón Mahuida pass, seven individual pillow lava vents are aligned in an ENE–WSW direction (Figs. 6A and B) directly over the trace of the Lomín fault (Fig. 3). These subglacial vents lie over a glacially eroded valley, which implies that they formed during the last glaciation. At least seven individual isolated vents with subglacial characteristics were also identified during the present survey inside the Caviahue caldera, aligned with the WNW-trending normal faults that form the Caviahue graben (explained in detail subsequently) (Figs. 3 and 4).

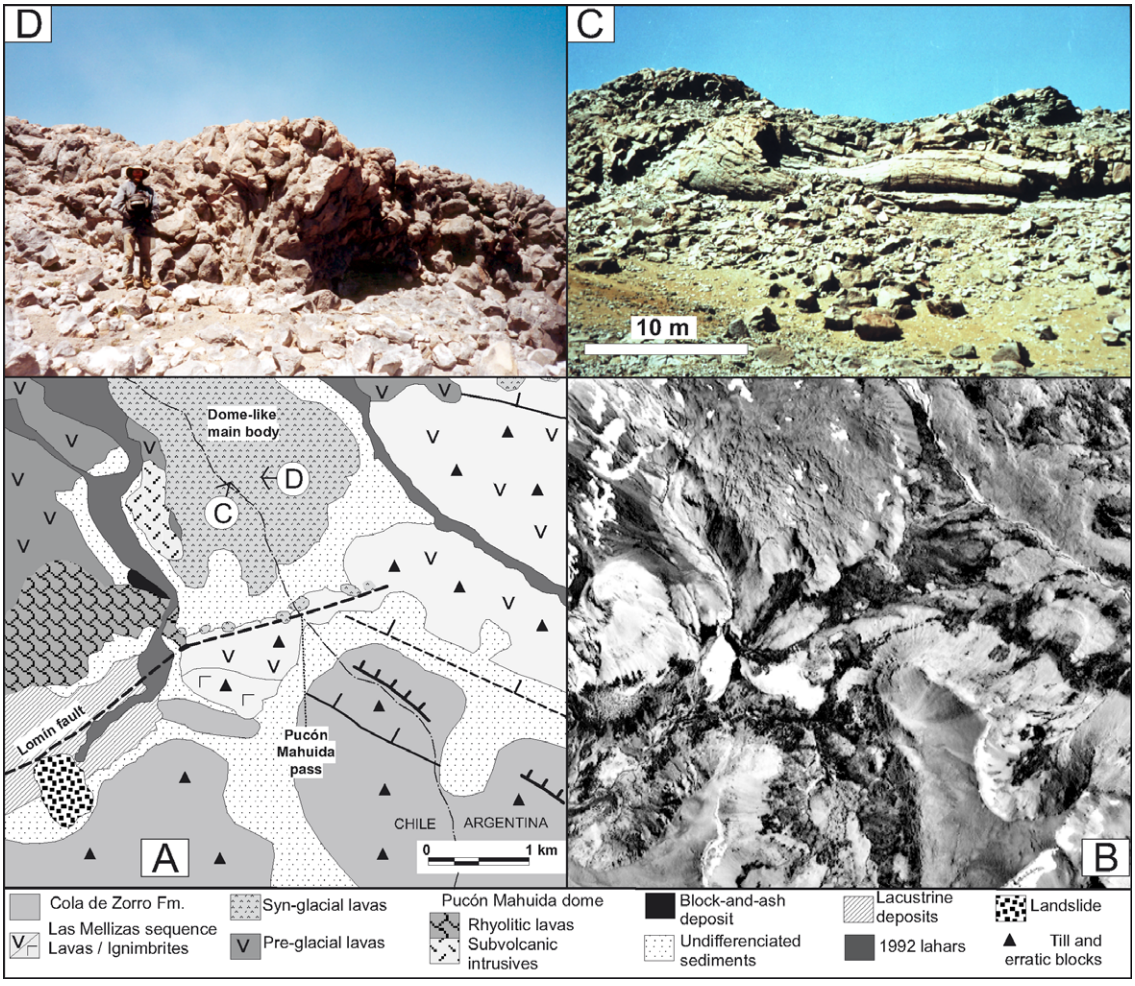

Fig. 6. Subglacial products of Copahue volcano. (A) Geologic map of the Pucón Mahuida pass area. See Fig. 3 for location. (B) SAF 1998 1:70,000 aerial photo of the same area as in (A). Isolated vents are aligned along the Lomín fault. Note the lack of glacial erosion on the dome-like main body of subglacial lavas on the northern part of the image, in contrast with the plateau on the southern part, which is polished by glacial abrasion. (C) Detail of a lava tube. (D) Detail of pillow lavas. For location, see (A).

3.5.3. Post-glacial stage 3

This stage is characterized by explosive emissions of relatively low volumes of lavas and pyroclastic flows erupted from summit craters, lateral fissures, and aligned monogenetic pyroclastic cones and vents (Figs. 3 and 7). On the northeastern part of the volcano, lava flows overlie moraine deposits that probably formed during the last glaciation. Massive pyroclastic deposits and minor lavas flank the north and west of the summit craters (Fig. 4). This stage is characterized by homogeneous basaltic–andesitic block lava flows of uniform composition (54.9–56.9% SiO_2, Cecioni et al., 2000). Five main identified emission centers may be chronologically grouped. Local names appear in Fig. 3 and numbers of the flows in Fig. 4.

1. Lava flows and related breccias emitted from a summit crater partially covered by ice. These flows extend for 18.6 km along the Lomín River Valley (Figs. 4, 7). The 1:20,000 scale color aerial photos show that these flows are affected by normal faults that form scarps up to 15 m high, with a dextral strike-slip component according to the several aligned, oblique secondary faults and offsets in the drainage network (Melnick, 2000).
2. Lavas emitted from four main vents along a 1.2 km long, N60°E-striking fissure on the eastern flank of the volcano. These flows extend for 5 km along the Copahue pass, where they are affected by normal faults, which also feed this lava field through at least five small aligned cones (Folguera and Ramos, 2000). The normal faults trend NE, forming southeast-facing scarps up to 10–15 m high. They also cut older lavas and unconsolidated glacial sediments (the scarps are visible on the aerial photo of Fig. 10B).
3. The Malla–Malla lavas were emitted from a series of at least four aligned pyroclastic cones and one crater partially covered by sediments, which form a 1.1 km long, N50°E-striking alignment. The flows extend for 5 km into the Lomín Valley and cover the flows described in (1) (Fig. 7).
4. Two small lava flows emitted from two vents on top of the subglacial dome-like body. The two vents are E–W aligned, and the flows are 2–3 m thick and extend eastward for 800 m.
5. At least two lava flows emitted from a crater north of the active Agrio crater. They are 3–5 m thick and extend northward for 850 m.

Fig. 7. Oblique aerial photo to the north of the Copahue volcano. Note the fault scarp and syncline to the right. The Malla–Malla aligned cones and extent of its lavas is shown. Arrows indicate flow direction. CHCO, Chancho-Có block; PM, Pucón Mahuida dome; 1992, Recent lahars. The volcanoes in the back are Sierra Velluda (left) and Antuco.

Several post-glacial pyroclastic flows are exposed around the Copahue volcano. In the southeastern flank, east of the Pucón Mahuida dome, a block-and-ash deposit is exposed (Fig. 6). This pyroclastic deposit covers at least five hectares with thicknesses of 1–2 m and is locally cut by small normal faults. In the Liay Valley, three pyroclastic flows interbedded in fluvial conglomerates are exposed in one section to form a terrace. These flows probably emitted from the western summit craters. Radiocarbon ages of these flows range from 2280 ± 50 to 2880 ± 50 years. BP (Cecioni et al., 2000; Polanco et al., 2000) (Fig. 4; Table 3). Inside the caldera, Polanco et al. (2000) report two more ^{14}C ages from pyroclastic flows of 8770 ± 70 and 5910 ± 50 years. BP (Fig. 4 and Table 3), probably emitted from the eastern craters. These ages and relations among the post-glacial lavas indicate that during the Holocene, the summit craters were intermittently active.

Historical deposits from the 1992 to 2000 eruptive cycle, mostly fallout, lahar deposits, juvenile bombs, and altered clasts, cover most of the eastern mouth of the Agrio crater (Fig. 8). The 1992 lahars were large, forming fans in the upper Agrio and Lomín rivers up to 3 m thick that contain blocks up to 5 m in diameter (Figs. 6 and 7). The 1992 crater lake eruption was characterized by the emission of altered rock fragments, siliceous dust, and copious amounts of green and yellow liquid sulfur (Delpino and Bermúdez, 1995). The June–October 2000 eruption ejected mostly pyroclasts ranging in size from ash to an 80 cm bomb found 300 m east of the Agrio crater. This episode was characterized by phreatomagmatic events (VEI 1–2, Global Volcanism Network, 2000a,b) ejecting altered rock fragments, siliceous white dust, liquid sulfur, and juvenile basaltic–andesitic fragments (Varekamp et al., 2001).

3.6. Pucón Mahuida dome

This dome is located on the southeastern slope of the Copahue volcano (Figs. 6 and 7). Two lithofacies were identified: rhyolitic lavas (72.8% SiO_2, Cecioni et al., 2000) that form the main body and rhyolitic subvolcanic

Table 3
Compiled ^{14}C ages of explosive products of the Copahue volcano

Sample N°	Locality	Analysis type	Type of material	^{14}C age years BP	Error ± years
BB-33B*	Liay river	Standard	Carbon	2280	50
B-33B*	Liay river	Standard	Carbon	2630	80
BB-89*	Caviahue lake	AMS	Carbon	5910	50
BB-84A*	Caviahue lake	Standard	Turba	8770	70
LL-A#	Liay river	Standard	Carbon	2880	50
LL-C#	Liay river	Standard	Carbon	2520	40
LL-F#	Liay river	Standard	Carbon	2460	40

Sources: *Polanco et al. (2000), #Cecioni et al. (2000). Sample locations in Fig. 4. BP, before present. Radiocarbon ages are conventionally specified to the year 1950, defined as present.

Fig. 8. Panoramic view to the south of the active Agrio crater and acid lake (125 m diameter, pH 0.3; Varekamp et al., 2001). Note the cover of black pyroclasts from the last eruption in 2000. The glacier that feeds the lake with meteoric waters appears on the right side; note the layers of pyroclastic deposits in the glacier.

intrusive rocks that crop out locally on the eastern side of the upper Lomín River (Fig. 4). The intrusive rocks are exposed due to glacial erosion along this valley. Sills coming out of the main body intrude andesitic lavas of the lower Copahue volcano edifice, but the upper part of the same lavas cover the dome. K–Ar ages from the Pucón Mahuida dome of 0.9 ± 0.14 and 1.1 ± 0.18 Ma (Linares et al., 1999) and 1.23 ± 0.18 to 0.76 ± 0.14 Ma (Muñoz and Stern, 1988; Linares et al., 1999) from andesites at the base and top of the Copahue edifice, respectively, are consistent with these field observations. Rhyolitic lavas from this dome are in contact by the Lomín fault with ignimbrites from Las Mellizas volcanic sequence in the Pucón Mahuida pass (Fig. 6A).

3.7. Cerro Bayo dome

Pesce (1989) identifies this body as a dome composed of dacitic to rhyolitic lavas and tuffs. It is located in the northern edge of the Caviahue caldera, covers an area of 20 km^2, and is approximately 1300 m higher than the caldera border (Figs. 3 and 4). Linares et al. (1999) report one K–Ar age of 0.6 ± 0.12 Ma for a rhyolitic lava. Its main conduit is emplaced at the crossing of the normal faults of the Caviahue caldera border and a NNE-trending fault, which bounds the western part of the dome and represents the southernmost extension of the Copahue–Antiñir fold-and-thrust system (Figs. 2 and 3).

4. Structures of the Caviahue–Copahue complex

4.1. Lomín fault

This NE-trending fault is parallel to the Lomín River for approximately 25 km, ending at the southwestern border of the Caviahue caldera. The Lomín fault can be considered the main fault of the horsetail-like array formed at the north end of the LOFZ. It limits a higher block to the

southeast, with elevations reaching 2000–2300 m. This block is formed by a northwest-facing asymmetric anticline exposing 800 m of the Cura-Mallín and 400 m of the Trapa–Trapa formations, unconformably covered by 100 m of horizontal Pliocene lavas of the Cola de Zorro Formation. The area northwest of the Lomín fault has lower mean elevations of 1600–1800 m, without considering the Copahue volcano, and is formed by a minimum of 200 m of folded Cura-Mallín strata covered by horizontal volcanic rocks of Las Mellizas sequence. The Trapa–Trapa unit is formed by thick beds of conglomerates and breccias and minor lavas and pyroclastic rocks. The geometry of the asymmetric anticline exposing the Oligo–Miocene units south of the Lomín fault, the absence of the Trapa–Trapa formation to the north, and its coarse clastic deposits to the south indicate that the Lomín fault was a normal fault, active during the deposition of the Trapa–Trapa unit and later inverted during late Miocene time prior to the deposition of the Cola de Zorro Formation.

A late Miocene andesitic porphyry intrudes the Cura-Mallín and Trapa–Trapa formations (Fig. 4). The porphyry is emplaced in an eastward-bending segment of the fault, which produced an extensional jog that may have facilitated magma emplacement. Small subsidiary faults with subhorizontal striations are exposed in the southern block, striking parallel to the main Lomín fault (Fig. 3). At Pucón Mahuida pass, the Lomín fault juxtaposes rhyolites from the Pucón Mahuida dome with ignimbrites from Las Mellizas sequence, forming a 1 m wide, vertical cataclastic zone.

Neotectonic activity along the Lomín fault is evidenced by fault scarps cutting Holocene lavas from the Copahue volcano (Melnick, 2000) (Fig. 3). The Holocene lava sequence is about 20–25 m thick, as observed in river-incised profiles. The faults on the Holocene lavas are 300–1000 m long and form scarps up to 5–10 m high. The drainage network above the Holocene lavas is locally controlled by these faults that produce small offsets and high-angle breaks in the main river. The faults clearly cut the cooling fabric of the lava flows and the Pliocene Las Mellizas sequence.

4.2. Structure of the Caviahue caldera

The Caviahue caldera is a rectangular, 15×20 km depression located in the central part of the CCM lineament (Fig. 2A). Groeber (1921) was the first to identify and describe this depression, but González-Ferrán (1978, in González-Ferrán, 1994) was the first to suggest a volcanic origin. In the present work, we consider LandSat ETM+ images, a digital elevation model based on the SRTM-Nasa dataset, published regional structural data, and strike-slip focal mechanism solutions from crustal earthquakes to interpret the Caviahue caldera as controlled by a pull-apart structure formed by dextral displacements along the northern LOFZ (Fig. 2A). The main evidence for this hypothesis is as follows:

(1) The caldera is limited by two major fault zones, the Copahue–Antiñir thrust system to the north and the Lomín fault, the main branch of the northern LOFZ, to the south (Fig. 2A). The LOFZ has good evidences of Plio–Quaternary dextral kinematics (e.g., Lavenu and Cembrano, 1999; Potent and Reuther, 2001; Potent, 2003; Rosenau, 2004; Melnick et al., 2006). Strike-slip focal mechanisms from crustal earthquakes located above or close to the main trace of the LOFZ have been reported (Chinn and Isacks, 1983; Barrientos and Acevedo, 1992; Reinecker et al., 2004).
(2) The Caviahue caldera is located at an inflection point of the LOFZ, where pull-apart structures are observed along other intra-arc fault zones (Sieh and Natawidjaja, 2000; Burbank and Anderson, 2001).
(3) Two NE-trending half-grabens with opposite polarity are located approximately 10 km to the north and the same distance south of the Caviahue caldera, along the Damas and Chaquilvín valleys, respectively (Fig. 2A). The tilting of the Pliocene lavas in the hangingwall, up to 30° in the northern half-graben, exposes folded Oligo–Miocene rocks in the footwall of both half-grabens. The rectangular Caviahue caldera and these two half-grabens form a symmetrical arrangement with the caldera in its center (Fig. 2A).
(4) The shape of volcanic calderas is generally circular to elliptic (Lipman, 1997). Square or rectangular calderas are observed along volcanic arcs associated with crustal-scale strike-slip faults where they are controlled by pull-apart structures, as observed along the Great Sumatran fault (Sieh and Natawidjaja, 2000) and North Luzon block (Pubellier et al., 2000).

The sedimentary deposits observed at the base of Las Mellizas volcanic sequence, the first post-caldera unit, probably represent the sedimentary infill of the pull-apart structure due to subsidence of the central block. On the southwestern part of the Caviahue caldera, a low-angle thrust fault truncates Pliocene volcanic rocks of the Cola de Zorro Formation and forms a syncline in the hangingwall. This fault strikes NW–SE and forms an approximately 100 m high fault scarp, which is eroded by glacial cirques to the southeast (Figs. 3 and 7). We posit this fault accommodated deformation during opening of the pull-apart structure. On the basis of these arguments, we consider the Caviahue caldera formed as a volcanic structure with a strong structural control.

4.3. El Barco structural system

El Barco Lake is a N–S-elongated, 4×1 km depression, located in a hanging position approximately 100 m higher than the Pelahuenco and Treputreo rivers (Fig. 9A) with no expression of surface drainage. This area is formed by subhorizontal late Pliocene basaltic lavas from Las Melli-

zas volcanic sequence (Figs. 4, 9A). El Barco Lake was formed by the damming of a glacial valley at its southern part. The dam is formed by basaltic lavas covered by Quaternary semiconsolidated conglomerates and cross-bedded sandstones of fluvial origin, which both dip 40°W, as observed at a gravel quarry on the access road to the southern part of the lake. The dam has an asymmetric double-ridge morphology with a steeper slope on the eastern side, seen in the digital elevation model and aerial photo shown in Fig. 9. The fluvial deposits observed in the quarry crop out in a horizontal position on top of the lavas in the Vizcachas area (Fig. 9A) on the western side of the valley, 300 m higher than at the quarry. The morphology of the dam and west dip of the lavas and fluvial deposits indicate a westward tilting of the block damming the lake. On the western part of the dam, a concave to the east scarp, seen in the aerial photo (Fig. 9B), is related to the block tilting, which is interpreted as produced by a normal fault.

Along the upper Treputreo River, a 3 km long, N–S-trending fault scarp was identified in the field and clearly visible in the aerial photo (Fig. 9B). The scarp has a concave to the east trace and is almost uneroded. The shore of the lake and base of the Treputreo River represent a geomorphic marker in the former flat bottom of the glacial valley. On the basis of this observation, we posit that an east-down normal fault produced this scarp. The scarp is 35 m high in the central part and decreases in elevation northward. The lack of erosion in the scarp, unexpected in the humid climate of the region, and its position offsetting the bottom of a glacial valley indicate late Quaternary activity along this fault. East-down normal faults continue to the south along the Treputreo River, exposing the Cura-Mallín Formation on the footwall (Fig. 4). Another 1.5 km long, concave to the east fault scarp affects the basaltic lavas, forming a westward-tilted block at Puesto Quemado. On top of this block, Sapo Lake (Fig. 9A) is bounded by a normal fault and interpreted as a sag pond related to the normal faulting and block tilting in the area. These observations indicate late Quaternary, E–W extension in El Barco.

4.4. Caviahue and Trolope grabens

Caviahue Lake has a horseshoe-like shape, formed by two 10 km long, 4 km wide arms limited by a central ridge (Fig. 3). In the surroundings of the lake, several WNW-trending normal faults cut Las Mellizas sequence and andesites from the base of the Copahue volcano. The faults have a strong topographic expression that controls the elongated shape of Caviahue Lake and the stair morphology of the western valleys, as the digital elevation model (Fig. 3) shows. Around the lake, ignimbrites and basaltic lavas from Las Mellizas sequence are juxtaposed by WNW-trending normal faults (Fig. 4). The normal faults form a horst-and-graben structure that controls the horseshoe morphology of Caviahue Lake, with the horst forming the ridge in the central part of the lake. Small fault-bounded bedrock lakes formed on the shoulders of the graben. East of Caviahue Lake, two faults cut the Cola de Zorro Formation on the eastern wall of the Caviahue caldera (Fig. 3) and limit a central block where the border of the caldera is downthrown by approximately 150 m, indicating normal faulting.

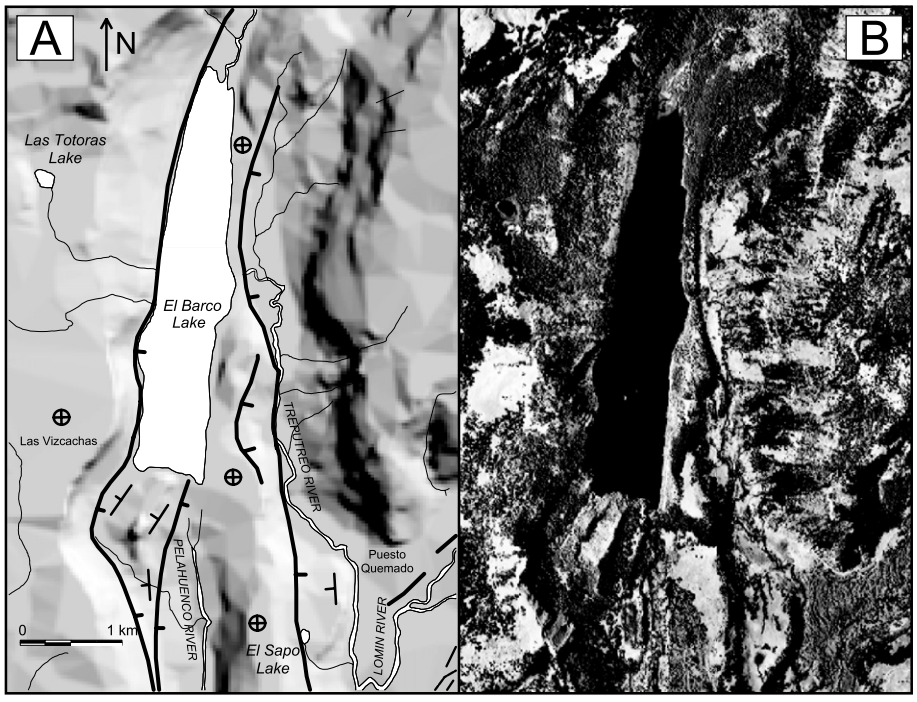

Fig. 9. Holocene normal faulting at El Barco. (A) Shaded-relief digital elevation model generated from 1:50,000 topomaps, river network (thin lines), and structural interpretation. (B) SAF 1998 1:70,000 scale aerial photo. Note concave fault scarps surrounding the lake with no significant erosion.

Isolated eruption centers of pillow lavas from Copahue stage 2 are aligned along the faults from the northern part of the graben (Fig. 4). The northern fault of the Caviahue graben was first identified during geothermal exploration studies (Dellapé and Pando, 1975) and used as a target zone for the three 1000 m deep geothermal wells (Fig. 3). This graben was formed after the opening of the Caviahue caldera, affecting the Pliocene–early Pleistocene units. The topographic expression of the graben and emplacement of synglacial products along the northern graben-bounding faults also might indicate late Pleistocene activity.

The northern part of the Caviahue caldera is characterized by an E–W-elongated depression (Fig. 3). In this area, normal faults juxtapose the basal lavas from Las Mellizas sequence with ignimbrites from the same unit, volcanic breccias from the Cola de Zorro Formation, and 1.6–0.8 Ma old andesites from the Trolope flows (Fig. 4). A fault-bounded block of ignimbrites hangs on the northern wall of the Caviahue caldera, and these same rocks constitute the floor of the valley in Trolope (Fig. 4). The normal faults form a half-graben structure, where the main fault is the Trolope fault (Fig. 3), and secondary faults formed along the northern border of the Caviahue caldera and on the floor of the valley. The Trolope fault trends E–W, with north-down polarity, and exposes the Cola de Zorro Formation along its footwall. A minimum of 200 m of vertical displacement during the last 2.6 Myr is estimated for this fault, with the surface of the ignimbrites from Las Mellizas sequence as a geomorphic marker (Fig. 4). We propose that the Trolope flows used the normal faults of the caldera border and possibly the Trolope fault as a main passage, filling a structurally controlled depression. The ignimbrites on the bottom of the valley are generally subhorizontal, but in some areas close to the Trolope fault, they are tilted up to 25°S.

The general strike of the Caviahue and Trolope grabens is parallel to the long axis of the rectangular Caviahue caldera. The NNE–SSW-oriented axis of extension of both grabens is compatible with the opening of the caldera pull-apart structure and the local stress field inside the caldera. Therefore, we interpret the Caviahue and Trolope grabens as caused by reactivations of the Caviahue caldera pull-apart structure during late Pliocene–Pleistocene times and in response to dextral shear along the LOFZ.

4.5. Chancho-Có structure

A ridge elongated in a NE–SW direction is located in the central to northwestern sector of the Caviahue caldera (Fig. 3). The morphology and position of this ridge inside the caldera can be considered a typical resurgent dome, as observed in many volcanic-related calderas and analogue modeling (e.g., Acocella et al., 2001, 2004); however, a detailed reconnaissance of the area suggests a tectonic origin or a strong structural control on resurgence.

The core of this structure is formed by slightly tilted volcanic breccias and lavas from the Cola de Zorro Formation, exposed along the Copahue pass and inside the Anfiteatro and Copahue town depressions (Figs. 3, 10B, 11). Covering these deposits in erosional unconformity is a 5–10 m thick ignimbrite from Las Mellizas sequence, dated at 2.6 ± 0.2 Ma, whose surface was polished by glacial erosion. Folguera and Ramos (2000) describe reverse faults and folds that affect the ignimbrite and generate spectacular fault-scarps up to 8 m high (Fig. 10D) and open cracks (Fig. 10C) that cut the glaciated surface. This contractional structure is formed by two main N60°E-striking, southeast-vergent, reverse faults that propagate two anticlines on the respective hangingwalls (Figs. 10B and 11). The southern fault marks the main topographic break inside the caldera, thrusting the ignimbrite over Quaternary till-like deposits, as observed in a quarry near the town of Copahue (Folguera and Ramos, 2000). The anticlines plunge to the northeast, and the offset along the reverse faults decreases in the same direction. The vertical displacement of the unconformity between Cola de Zorro and the ignimbrite is approximately 30 m, estimated at the locality shown in Fig. 11. In contrast, the post-glacial scarp of this fault, which offsets the surface of the ignimbrite polished by glacial abrasion, is only 4–5 m high. These observations indicate that the Chancho-Có structure was active during the Pleistocene and Holocene. The Chancho-Có faults control the main active geothermal conducts in the area, Copahue town, Anfiteatro, and Las Maquinitas hot springs, which form an en échelon arrangement (Figs. 10A and B).

Extensional faults and open cracks (Figs. 10B and C) are exposed along the axis of the anticlines forming fault scarps up to 3 m high. These normal faults and open cracks define small crestal grabens that trend slightly oblique to the reverse faults and the axis of the anticlines. The open cracks extend for tens of meters, reaching depths of 15 m, and are filled with small amounts of pyroclastic deposits that indicate a young age. These extensional features accommodate the bending-moment tensional stress related to the growth of the anticlines and were generated simultaneously with the compressive structure (.Burbank and Anderson, 2001). This finding is consistent with the position of the extensional structures in the area of higher contraction.

The Anfiteatro and Copahue town geothermal zones are emplaced in two small rectangular depressions of approximately 0.5 km^2. In some areas, exposed normal faults bound these topographic lows. The few fault-slip data measured along the reverse fault scarps indicate oblique dextral transpressional motion, consistent with the en échelon arrangement formed by the Anfiteatro, Copahue, and Las Maquinitas depressions and the slightly oblique trend of the crestal grabens and open cracks with respect to the main reverse faults (Fig. 10B). These geometries indicate that the direction of shortening was oblique to the trend of the main contractional structure (Burbank and Anderson, 2001).

Generally, caldera-related resurgent blocks are affected by normal faulting, reflecting gravitational instability

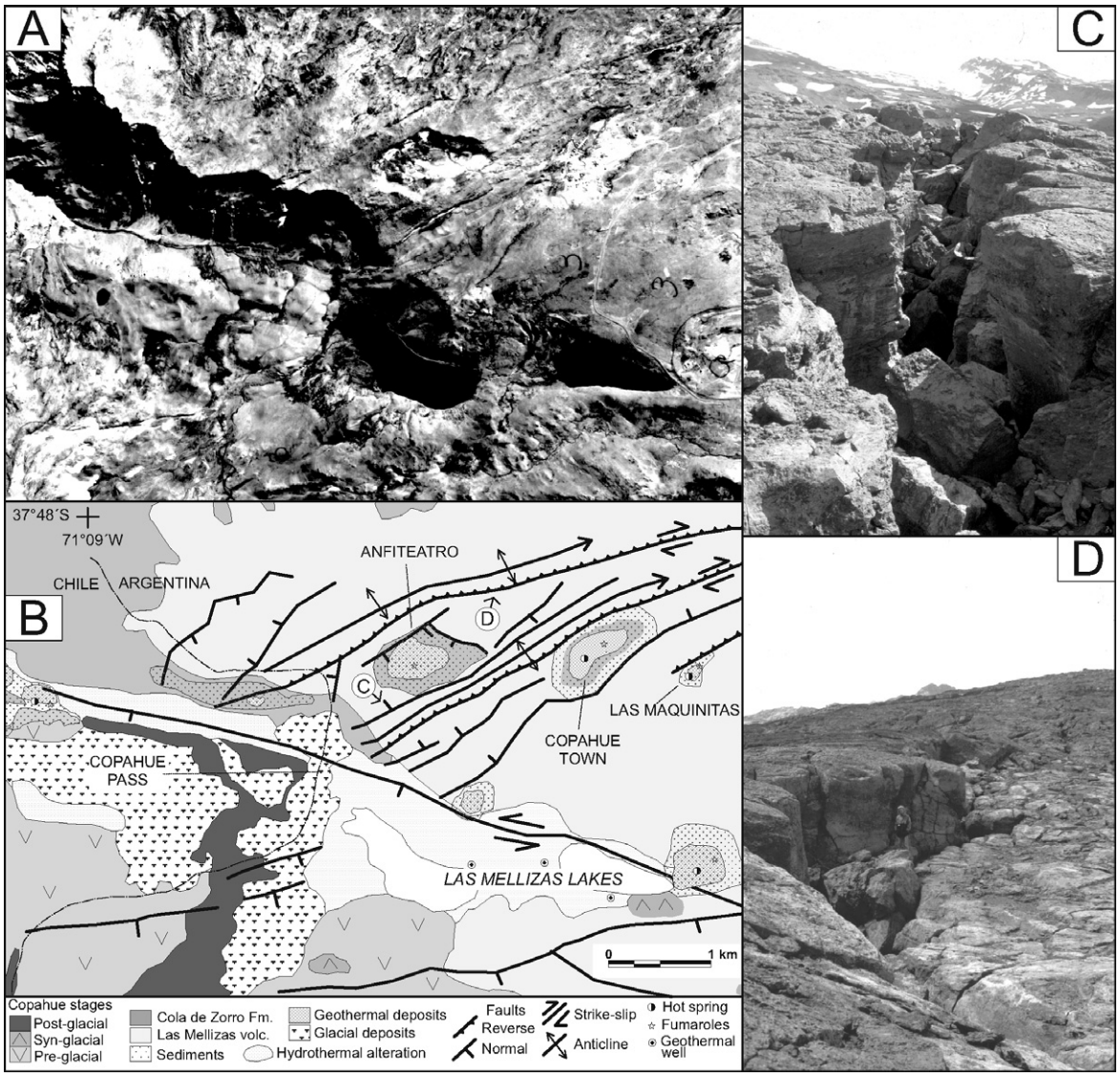

Fig. 10. Chancho-Có transpressive structure. (A) Aerial photo of Chancho-Có area. Note the NE-trending fault scarps at the center to upper right of the image, the en échelon depressions where geothermal activity concentrates, and the ENE-trending fault scarps on the lower left. (B) Geologic map of the same area as (A). (C) Detail view of an extensional open crack, located on the axis of the southern anticline. Crack is 3 m wide. (D) Detailed view to the northeast of the northern reverse fault scarp. For location, see (B).

(e.g., Acocella et al., 2001). The described reverse faults in resurgent blocks and observed in analogue modeling generally bound the block in its lowermost regions and accommodate the lack of space inside the caldera as the resurgent dome grows, without following any specific trend (Acocella et al., 2004). In contrast, the compressive structures at Chancho-Có are located on the upper part of the block. Moreover, the general N60°E strike of this structure is aligned with the post-glacial fissural effusions of the Copahue volcano (Fig. 3), the Holocene fault scarps on the eastern slope of the volcano (Figs. 10A and B), and, more important, a regional structure, the CCM transfer zone. Therefore, the Chancho-Có transpressive structure clearly developed under tectonic control; however, the role of resurgence is unknown.

We favor tectonic control in the development of Chancho-Có transpressive structure, but we cannot discard the possibility that structurally controlled caldera resurgence occurred in this system.

5. Structural control on magmatic and hydrothermal effusions: Role of regional and local structures

An extensional tectonic regime seems the most suitable for facilitating magma ascent to the surface. In this case, $\sigma_1 = \sigma_{\text{vertical}}$, and the forces acting on the horizontal plane are of lower magnitudes, $\sigma_3 = \sigma H_{\text{min}}$ and $\sigma_2 = \sigma H_{\text{max}}$, or the least and greatest horizontal principal stresses, respectively (e.g., Pasquarè and Tibaldi, 2003). Several studies document cases in which fissure eruptions and dykes can

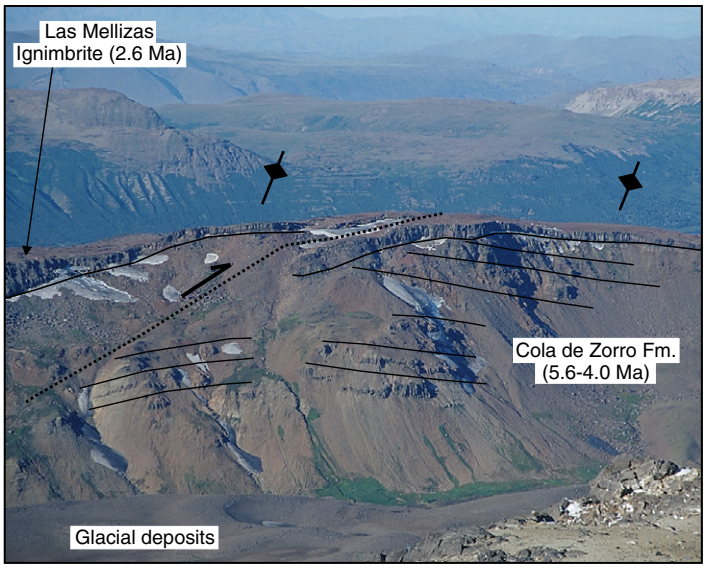

Fig. 11. View to the northeast of the Chancho-Có uplifted block from top of Copahue volcano illustrating the northern reverse fault (see Fig. 10B). Note the offset of the unconformity between the Cola de Zorro Formation and the ignimbrite from Las Mellizas volcanic sequence is approximately 30 m. The offset of the top of the ignimbrite polished by glacial abrasion is around 5 m (see Fig. 10D). Note the two anticlines flanking the fault. In the back, the border of the Caviahue caldera and, in the right corner, the Cerro Bayo dome can be seen.

be injected on both a local and a regional scale in a compressional regime ($\sigma_1 = \sigma H_{max}$), (e.g., Pasquarè et al., 1988; Tibaldi, 1992; Marra, 2001), so volcanism can occur with σ_1 and σ_3 acting on the horizontal plane, implying that magma pressure $\sigma_{mp} > \sigma H_{max}$.

The Patagonian Andes (38–47°S) experienced Plio–Quaternary dextral strike-slip faulting along LOFZ-related faults (e.g., Lavenu and Cembrano, 1999; Rosenau et al., 2006). Holocene tectonic activity is evident from strike-slip focal mechanisms of crustal earthquakes located near the main trace of the LOFZ (Chinn and Isacks, 1983; Barrientos and Acevedo, 1992; Reinecker et al., 2004); groups of elongated post-glacial pyroclastic cones aligned along LOFZ-oblique fractures, interpreted as synthetic or antithetic secondary structures (López-Escobar et al., 1995; Rosenau, 2004); and locally the dextral offset of Holocene landforms (Melnick et al., 2006). In the Patagonian Andes, Quaternary σH_{max} is oriented ENE to NE, close to the plate convergence direction (Lavenu and Cembrano, 1999; Reinecker et al., 2004). South of Copahue, between 38° and 39°S, Potent (2003) proposes a transtensional regime based on the inversion of fault-slip data measured on Plio–Pleistocene rocks, implying that $\sigma H_{max} = \sigma_1$ or σ_2 and that σ_3 is vertical. This proposal is consistent with geomorphological observations along the Lonquimay structure, a half-graben with a dextral strike-slip component on the main west-dipping fault. Strike-slip deformation is evident from the consistent dextral offsets of several ephemeral post-glacial streams (Melnick et al., 2006).

In the southwestern part of the CCM lineament, the perfect tension-gash geometry of the Callaqui volcano (Fig. 2D) defines a N60°E direction for σH_{max} during Quaternary times. In the tension-gash case, $\sigma H_{max} = \sigma_1$ and is perpendicular on the horizontal plane, $\sigma H_{min} = \sigma_3$, and, as expected, magmatic effusions are emplaced along a plane perpendicular to σH_{min}. In the northeastern part of the CCM, in the Mandolegüe range, dyke swarms, aligned cones, sector collapse of small stratovolcanoes, and the strike of normal faults have a similar trend, so the same stress field is proposed (σH_{max} = N60°E; σH_{min} = N30°W). In contrast, in the central part of the CCM, within Copahue and its surroundings, the structures have different kinematics that reflect an heterogeneous stress field, as determined using the orientation and geomorphology of Quaternary faults and the criteria proposed by Nakamura (1977) for the alignment of volcanic features, here of late Pleistocene–Holocene age (Fig. 12). Within the Caviahue–Copahue complex, most structures are extensional or transtensional, $\sigma H_{max} = \sigma_3$ or σ_2; compressional and transpressional structures that imply $\sigma H_{max} = \sigma_1$ develop only locally.

Along the CCM, as depicted in Fig. 12, the stress field at Callaqui volcano and Mandolegüe range is in accordance with the regional ENE–NE orientation of σH_{max}. In contrast, the stress field in the Copahue area is heterogeneous, and a progressive eastward clockwise rotation of σH_{max} is observed (Fig. 12). What controls the local heterogeneous stress field in Copahue and inside the Caviahue caldera? The horsetail-like geometry of the northern LOFZ is formed by splays, like the Lomín fault and El Barco system. The traces of these splays bend eastward, similar to the alignment of post-glacial cones and fissures of the Copahue volcano. Therefore, we propose that Copahue is rooted in an eastward-bending tailcrack that forms part of the fault array with horsetail geometry of the northern LOFZ. This scenario would explain the rotation of σH_{max}

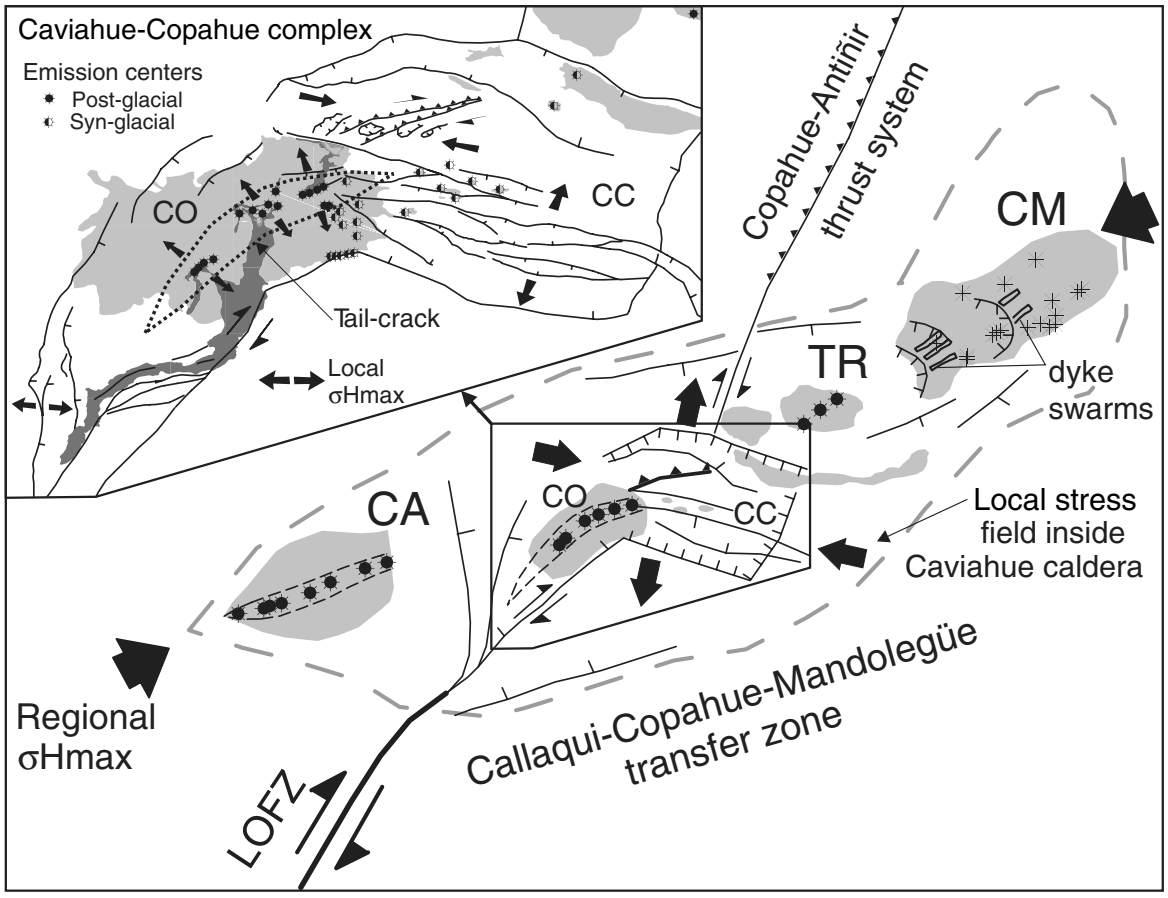

Fig. 12. Structural model of the Callaqui–Copahue–Mandolegüe transfer zone and Caviahue–Copahue complex. The black arrows indicate the direction of σH_{max}. Note the continuous clockwise rotation in the Copahue volcano (CO) and inside the Caviahue caldera (CC). We propose that Copahue is rooted in a tailcrack, part of the horsetail-like structure formed at the end of the Liquiñe-Ofqui fault zone. The local stress field inside the Caviahue caldera is formed by the interaction between the Callaqui–Copahue–Mandolegüe transfer zone, the Liquiñe-Ofqui fault zone, and the Copahue–Antiñir thrust system. CA, Callaqui volcano; TR, Trolón eruptive center; CM, Cordillera de Mandolegüe.

along the Copahue volcano, but what about inside the Caviahue caldera? The Caviahue and Trolope grabens are post-caldera extensional features limited to the interior of the caldera. The Caviahue graben has isolated late Pleistocene subglacial volcanic centers aligned along WNW–ESE-oriented normal faults, and extensive Pleistocene effusions are associated with the Trolope graben. These systems imply a NNE–SSW-oriented σH_{min} and WNW–SSE σH_{max}, which differ from the regional NE–SW-oriented σH_{max} (Fig. 12). As we mention previously, we propose that these two extensional systems are related to reactivations of the Caviahue caldera pull-apart structure and therefore reflect the local stress field inside the caldera. Moreover, this area represents interference among three regional structures: the Lomín fault, the main branch of the LOFZ; the CCM lineament; and the Copahue–Antiñir thrust system. In this area, local structures that develop at the intersection of the regional fault systems control the volcanic effusions, and we propose that this intersection controls the local heterogeneous stress field. The two rhyolitic domes of the complex are emplaced at the intersection of regional and local structures: the Bayo dome at the crossing of the Copahue–Antiñir thrust system and the northern normal faults of the Caviahue caldera, and the Pucón Mahuida dome at the crossing of the southern caldera border faults and the Lomín fault (Fig. 4). Both domes are emplaced at the border of the caldera, in areas where the stress field changes from regional to local, and bounded by a regional fault. This structural setting probably influenced the emplacement of acid magmatism.

No magmatic effusions but most of the hydrothermal activity and hot springs of the area concentrate along the transpressional Chancho-Có system. In this case, $\sigma_1 = \sigma H_{max}$, which is at a high angle to the fault planes. Most hydrothermal activity in this system is emplaced in small, extensional, en échelon depressions interpreted as hinge grabens related to the transpressional structure. These small extensional depressions are shallow features and do not reflect the stress field of the transpressional system. Therefore, the stress field can change close to the surface, and under local compression, hydrothermal fluids find the easiest passage when they are close to the surface and concentrate there.

In this region, the 90 km long CCM is the main structure that controls volcanic effusions at a regional scale. At a smaller scale, magmatic and hydrothermal effusions are

controlled by local structures, their geometries and kinematics, and their interaction with the regional fault systems.

6. Regional tectonic implications

Important consequences for regional tectonics can be extracted from the study of this volcanic complex. Between approximately 5 and 1 Ma, the volcanic products of the Cola de Zorro Formation, Las Mellizas volcanic sequence, and the base of Copahue volcano evolved during a first stage located at the corresponding active volcanic front (Muñoz and Stern, 1988). After the westward shifting of this volcanic front around 1 Ma (Muñoz and Stern, 1988; Lara et al., 2001), while most of the volcanic complexes located at the ancient Pliocene–lower Pleistocene volcanic front extinguished, Copahue survived. Although the cause for this anomalous behavior could be related to several factors, we favor a tectonic explanation.

We propose that the heterogeneous strain patterns and long-lived volcanism observed in the Caviahue–Copahue complex are related to the intersection of three regional structural systems: the CCM volcano-tectonic lineament, the Liquiñe-Ofqui strike-slip system, and the Copahue–Antiñir thrust system. The CCM structure evolved throughout the late Oligocene and Miocene as a transfer zone in the rifting and inversion phases of the Cura-Mallín Basin (Radic et al., 2002; Melnick et al., 2002) and is therefore a crustal-scale discontinuity. After the Pliocene, this structure continued as a transfer zone at the boundary between the strike-slip LOFZ and the compressive Copahue–Antiñir thrust system (Fig. 12), accommodating the step configuration of these two regional fault systems and decoupling their contrasting kinematics. This transfer zone, which controls the longest volcanic alignment of the southern volcanic zone is, according to our interpretation, controlled by a long-lived inherited discontinuity. Volcanic effusions in this area are controlled by the regional stress field imposed by plate convergence and a local stress field that develops at the intersection of regional structures.

The recurrence of volcanic activity in the Caviahue–Copahue complex is related, according to our hypothesis, to a crustal-scale weakness zone that accounts for a long-lived structural process, namely the strain transfer between the LOFZ and Copahue–Antiñir fault system. This explanation clarifies why localized, continuous, late Pleistocene–Holocene volcanic activity persisted only here along the Pliocene–lower Pleistocene volcanic front.

7. Evolution of the Caviahue–Copahue complex

The volcanic and structural evolution of the Caviahue caldera Copahue volcano complex may be summarized in five main stages, as depicted in Fig. 13:

(1) Opening of the Caviahue caldera pull-apart structure and related half-grabens during late Pliocene times, associated with the dextral LOFZ.
(2) Establishment of Las Mellizas basaltic–andesitic volcano and subsequent collapse during late Pliocene time. This collapse produced ignimbritic flows that filled the caldera and extended to the west.

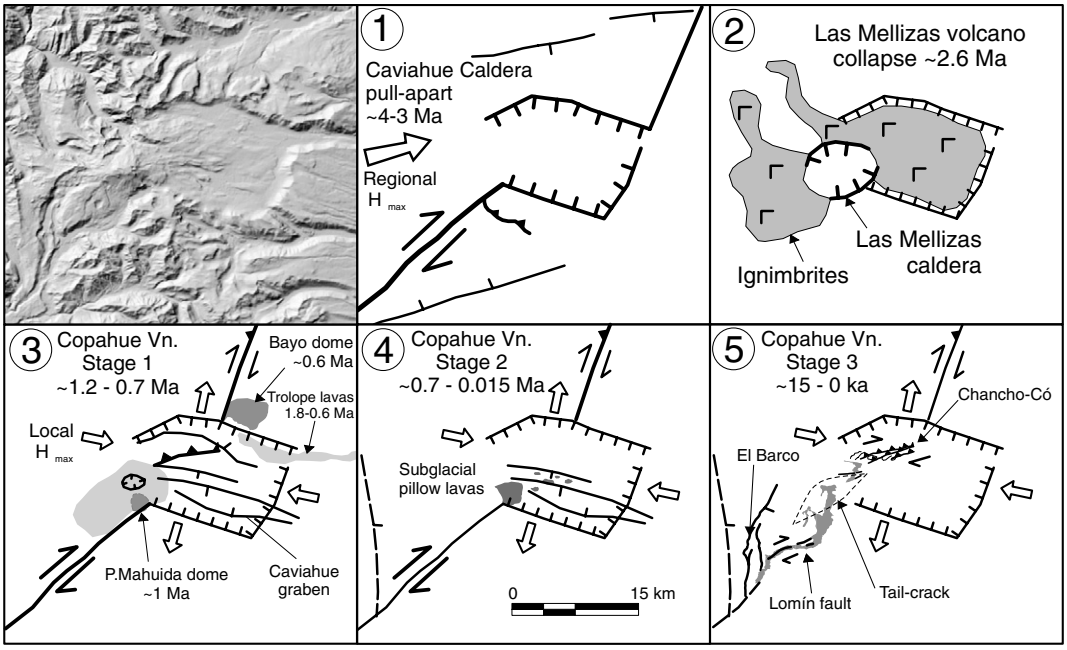

Fig. 13. Evolution of the Caviahue–Copahue complex. Upper left, Shaded-relief elevation model based on SRTM-Nasa data. (1) Opening of the Caviahue caldera pull-apart. (2) Establishment of Las Mellizas volcano and subsequent collapse, showing the resulting caldera and extent of ignimbrites. (3) Copahue volcano stage 1, emplacement of the Pucón Mahuida and Bayo ryholitic domes, opening of the Caviahue and Trolope graben, and effusion of the Trolope flows. (4) Copahue stage 2, eruption of andesitic–dacitic subglacial pillow lavas. (5) Copahue stage 3, eruption of basaltic–andesitic flows, and activation of faults with horsetail geometry and the tailcrack where Copahue is rooted.

(3) Establishment of the andesitic Copahue volcano at approximately 1.2 Ma. Reactivation of the Caviahue caldera pull-apart, which resulted in the opening of two intracaldera grabens and related volcanic effusions along graben bounding faults between 1.6 and 0.8 Ma. Emplacement of the Cerro Bayo and Pucón Mahuida rhyolitic domes at 0.6 and 1 Ma, respectively. Transpression and uplift of the Chancho-Có block in the center of the caldera.
(4) Late Pleistocene effusion of andesitic–dacitic subglacial pillow lavas forming the main, dome-like body on the southeastern flank of Copahue volcano; effusions along fault-controlled aligned centers.
(5) Holocene effusions of basaltic–andesitic lavas and pyroclastic flows from summit craters, lateral fissures, and aligned cones. Reactivation of reverse faulting and folding along the Chancho-Có block, extensional deformation in El Barco, and transtension along the Lomín fault.

8. Conclusions

At regional scale, Quaternary volcanism concentrates along the Callaqui–Copahue–Mandolegüe lineament, which is the longest volcanic lineament of the southern volcanic zone. We interpret this structure as an inherited crustal-scale transfer zone from the Oligo–Miocene Cura-Mallín rift Basin.

At a local scale, effusions are controlled by local structures formed at the intersection of regional fault systems.

Magma ascent occurs along planes perpendicular to the least principal horizontal stress (σH_{min}); hydrothermal activity and hot springs occur along planes perpendicular to the greatest horizontal stress (σH_{max}).

The persistence of volcanism in the Caviahue–Copahue complex during late Pleistocene–Holocene times in an "extinct" position of the former Pliocene–early Pleistocene volcanic front and the heterogeneous strain patterns observed in the complex are associated with the Callaqui–Copahue–Mandolegüe transfer zone. This structure decouples the strike-slip Liquiñe-Ofqui fault zone from the Copahue–Antiñir thrust system and represents the transition from the Central to the Patagonian Andes.

Acknowledgements

This work has benefited from the following projects: DAAD IQN at University of Potsdam, PIP 4162 (Conicet) and PICT 059 for the "Study of the segment of normal subduction – 33° to 38°S," GeoForschungsZentrum Potsdam Southern Andes project, and SFB 267 "Deformation Processes in the Andes." DM is grateful to M. Strecker and O. Oncken for supporting his research. We thank G. Hermosilla, D. Iaffa, D. Yagupsky, S. Zlotnik, E. González-Díaz, J. Clavero, E. Godoy, D. Sellés, M. Rosenau, H. Echtler, V. Consoli, A. Sandoval, and P. Sruoga for their help in the field and fruitful discussions. Reviews of a previous version by J. Cembrano, J.M. Espíndola, and J. Muñoz, as well as journal reviewers L. Lara and Michael Ort, helped clarify the ideas presented in the text and improved the use of the English language. We also acknowledge the Universidad de Concepción, Chile, and the Universidad de Buenos Aires, Argentina, where the two first authors' theses, on which this work is based, were developed.

References

Acocella, V., Cifelli, F., Funiciello, R., 2001. The control of overburden thickness on resurgent domes: insights from analogue models. Journal of Volcanology and Geothermal Research 111, 137–153.

Acocella, V., Funiciello, R., Marotta, E., Orsi, G., de Vita, S., 2004. The role of extensional structures on experimental calderas and resurgence. Journal of Volcanology and Geothermal Research 129, 199–217.

Bahar, I., Girod, M., 1983. Contrôle structural du volcanisme indonésien (Sumatra, Java-Bali), application et critique de la méthode de Nakamura. Bulletin de la Société Géologique de France 25, 609–614.

Barrientos, S., Acevedo, P., 1992. Seismological aspects of the 1988–1989 Lonquimay (Chile) volcanic eruption. Journal of Volcanology and Geothermal Research 53, 73–87.

Beck, M.E., 1983. On the mechanism of tectonic transport in zones of oblique subduction. Tectonophysics 93, 1–11.

Bohm, M., Lüth, S., Echtler, H., Asch, G., Bataille, K., Bruhn, C., Rietbrock, A., Wigger, P., 2002. The Southern Andes between 36 and 40°S latitude: seismicity and average seismic velocities. Tectonophysics 356, 275–289.

Burbank, D.W., Anderson, R.S., 2001. Tectonic Geomorphology. Blackwell Science, United Kingdom, 274 pp.

Carpinelli, A., 2000, Análisis estratigráfico, paleoambiental, estructural y modelo tectono-estratigráfico de la cuenca de Cura-Mallín, VIII y IX Región, Chile, Provincia de Neuquén, Argentina. Master's thesis, Universidad de Concepción, 158 pp.

Cashman, S.M., Kelsey, H.M., Erdman, C.F., Cutten, H.N., Berryman, K.R., 1992. Strain partitioning between structural domains in the forearc of the Hikurangi subduction zone, New Zealand. Tectonics 11, 242–257.

Cecioni, A., Alfaro, G., Pincheira, M., Pineda, V., Arce, M., Cares, R., Reyes, M., Valenzuela, G., Melnick, D., 2000. Elaboración de Mapas Zonificados de Peligrosidad Volcánica. INGENDESA S.A. (Unpublished), Universidad de Concepción, 250 pp.

Cembrano, J., Hervé, F., Lavenu, A., 1996. The Liquiñe Ofqui fault zone: a long-lived intra-arc fault system in southern Chile. Tectonophysics 259, 55–66.

Cembrano, J., Schermer, E., Lavenu, A., Sanhueza, A., 2000. Contrasting nature of deformation along an intra-arc shear zone, Liquiñe-Ofqui fault zone, southern Chilean Andes. Tectonophysics 319, 129–149.

Cembrano, J., Lavenu, A., Reynolds, P., Arancibia, G., López, G., Sanhueza, A., 2002. Late Cenozoic transpressional ductile deformation north of the Nazca-South America–Antarctica triple junction. Tectonophysics 354, 289–314.

Chinn, D.S., Isacks, B.L., 1983. Accurate source depths and focal mechanisms of shallow earthquakes in western South America and in the New Hebrides Island arc. Tectonics 2, 529–563.

Dellapé, D., Pando, G., 1975. Relevamiento geológico de la cuenca geotérmica de Copahue. Yacimientos Petrolíferos Fiscales (Unpublished), Informe 524, Buenos Aires.

Delpino, D., Bermúdez, A., 1993. La actividad volcánica del volcán Copahue durante 1992. Erupción con emisión de azufre piroclástico. Provincia de Neuquén. XII Congreso Geológico Argentino (Mendoza), Abstracts 4, 292–301.

Delpino, D., Bermúdez, A., 1995. Eruptions of pyroclastic sulphur at crater lake of Copahue volcano, Argentina. XXI International Union of

Geodesy and Geophysics (Boulder), General Assembly, Abstracts, B410.

Delpino, D., Deza, M., 1995. Mapa geológico y de recursos minerales de la Provincia de Neuquén, scale 1:500,000. Secretaría de Minería, Servicio Geológico Neuquino.

Dewey, J.F., Lamb, S.H., 1992. Active tectonics in the Andes. Tectonophysics 205, 79–95.

Fitch, T.J., 1972. Plate convergence, transcurrent faults, and internal deformation adjacent to southeast Asia and the western Pacific. Journal of Geophysical Research 77, 4432–4460.

Folguera, A., Ramos, V.A., 2000. Control estructural del volcán Copahue (38°S–71°O): implicancias tectónicas para el arco volcánico cuaternario (36–39°S). Revista de la Asociación Geológica Argentina 55, 229–244.

Folguera, A., Yagupsky, D., Zlotnik, S., Iaffa, D., Melnick, D., 2001. Transtensión como mecanismo de transición entre estados de baja y alta partición de la deformación entre 37°S y 40°S en el Plioceno y Cuaternario. XI Congreso Geológico Latinoamericano (Montevideo), electronic files.

Folguera, A., 2002. Evolución de una cuenca de intra-arco en una zona de subducción ante convergencia oblicua. Estudio comparativo de la cuenca Neógena Neuquina (37° y 39°S) y la cuenca Mesozoica de Río Mayo. Ph.D Thesis, Universidad de Buenos Aires, 257 pp.

Folguera, A., Ramos, V.A., Melnick, D., 2003. Recurrencia en el desarrollo de cuencas de intra-arco. Cordillera Neuquina (37°30′). Revista de la Asociación Geológica Argentina 58, 3–19.

Folguera, A., Ramos, V.A., Hermanns, R.L., Naranjo, J.A., 2004. Neotectonics in the foothills of the southernmost central Andes (37°–38°S): Evidence of strike-slip displacement along the Antiñir-Copahue fault zone. Tectonics 23, 1–23, TC5008.

Glazner, A.F., 1991. Plutonism, oblique subduction, and continental growth: an example from the Mesozoic of California. Geology 19, 784–786.

Global Volcanism Network, 2000a. Frequent ash explosions and acidic mudflows starting on July 1. Global Volcano Network Bulletin 25, 6.

Global Volcanism Network, 2000b. Continued ash explosions and tremor during August–October. Global Volcano Network Bulletin 25, 9.

González, O., Vergara, M., 1962. Reconocimiento geológico de la Cordillera de Los Andes entre los paralelos 35° y 38° S. Universidad de Chile, Instituto de Geología, Publicación 24, 119 pp.

González-Ferrán, O., 1994. Volcanes de Chile. Instituto Geográfico Militar, Santiago, 640 pp.

Groeber, P., 1921. La región de Copahue y su glaciación diluvial. Revista de la Sociedad Argentina de Estudios Geográficos 1, 92–110.

Hermanns, R., González-Díaz, E., Folguera, A., Mardones, M., 2003. Large massive rock slope failures, landslide dams, related valley evolution, and their association with the tectonic setting in the Argentine and Chilean Andes between 36 and 38°S. X Congreso Geológico Chileno (Concepción), electronic files.

Hervé, M., 1976. Estudio geológico de la falla Liquiñe-Reloncaví an el área de Liquiñe: antecedentes de un movimiento transcurrente (Provincia de Vadivia). I Congreso Geológico Chileno (Santiago), Abstracts B, 39–56.

Hervé, F., 1994. The southern Andes between 39° and 44°S latitude: the geological signature of a transpressive tectonic regime related to a magmatic arc. In: Reutter, K.J., Scheuber, E., Wigger, P.J. (Eds.), Tectonics of the Southern Central Andes. Springer, Berlin, pp. 243–248.

Hickey-Vargas, R., Moreno, H., López-Escobar, L., Frey, F.A., 1989. Geochemical variations in Andean basaltic and silicic lavas from the Villarica-Lanín volcanic chain (39.5°S): an evaluation of source heterogeneity, fractional crystallization and crustal assimilation. Contributions to Mineralogy and Petrology 103, 361–386.

Hildreth, W., Moorbath, S., 1988. Crustal contributions to arc magmatism in the Andes of central Chile. Contributions to Mineralogy and Petrology 98, 455–489.

Iaffa, D., González-Díaz, E., Folguera, A., 2002. Tectónica postglaciaria en la cordillera Neuquina. Río Picunleo (37°30′S). XIV Congreso Geológico Argentino (Calafate), electronic files.

JICA (Japan International Cooperation Agency), 1992. The feasibility study on the Northern Neuquén Geothermal Development Project. (Unpublished), Ente Provincial de Energia de la Provincial del Neuquén. 89 pp.

Lara, L., Rodríguez, C., Moreno, H., Pérez de Arce, C., 2001. Geocronología K–Ar y geoquímica del volcanismo plioceno superior-pleistoceno en los Andes del sur (39°–42°S). Revista Geológica de Chile 28, 67–91.

Lavenu, A., Cembrano, J., 1999. Compressional and transpressional stress pattern for Pliocene and Quaternary brittle deformation in forearc and intra-arc zones (Andes of Central and Southern Chile). Journal of Structural Geology 21, 1669–1691.

Lescinsky, D.T., Fink, J.H., 2000. Lava and ice interaction at stratovolcanoes: use of characteristic features to determine past glacial extents and future volcanic hazards. Journal of Geophysical Research 105 (B10), 23,711–23,726.

Linares, E., Ostera, H.A., Mas, L., 1999. Cronología Potasio-Argón del conplejo efusivo Copahue–Caviahue, Provincia de Neuquén. Revista de la Asociación Geológica Argentina 54 (3), 240–247.

Lipman, P.W., 1997. Subsidence of ash-flow calderas: relation to caldera size and magma-chamber geometry. Bulletin of Volcanology 59, 198–218.

López-Escobar, L., Cembrano, J., Moreno, H., 1995. Geochemistry and tectonics of the Chilean Southern Andes Quaternary volcanism (37°–46°S). Revista Geológica de Chile 22 (2), 219–234.

Lowell, T.V., Heusser, C.J., Andersen, B.G., Moreno, P.I., Hauser, A., Heusser, L.E., Schlüchter, C., Marchant, D.R., Denton, G.H., 1995. Interhemispheric correlation of late pleistocene glacial events. Science 269, 1541–1549.

Lüth, S.ISSA 2000 working group, 2003. A crustal model along 39°S from a seismic refraction profile- ISSA 2000. Revista Geológica de Chile 30, 83–101.

Marra, F., 2001. Strike-slip faulting and block rotation: a possible triggering mechanism for lava flows in the Alban Hills? Journal of Structural Geology 23, 127–141.

Martini, M., Bermúdez, A., Delpino, D., Giannini, L., 1997. The thermal manifestations of Copahue volcano area. Neuquén, Argentina. VIII Congreso Geológico Chileno (Antofagasta), Abstracts 1, 352–356.

Mazzoni, M.M., Licitra, D., 2000. Significado estratigráfico y volcanológico de ignimbritas neógenas con composición intermedia en la zona del lago Caviahue, Neuquén. Revista de la Asociación Geológica Argentina 55 (3), 188–200.

Melnick, D., 2000. Geometría y estructuras de la parte norte de la zona de falla de Liquiñe-Ofqui (38°S): interpretación de sensores remotos. IX Congreso Geológico Chileno (Puerto Varas), Abstracts 1, 796–799.

Melnick, D., Folguera, A., 2001. Geología del complejo volcánico Copahue - Caldera del Agrio, un sistema transtensional activo desde el Plioceno en la transición de los Andes Patagónicos a los Andes Centrales (38°S–71°O). IX Congreso Geológico Latinoamericano (Montevideo), electronic files.

Melnick, D., Folguera, A., Rosenau, M., Echtler, H., Potent, S., 2002. Tectonics from the Northern segment of the Liquiñe-Ofqui fault system (37°–39°S), Patagonian Andes. V International Symposium of Andean Geodynamics (Toulouse), Extended Abstracts, 413–417.

Melnick, D., 2004. Geología del Cuadrángulo Volcán Copahue (38°S, 71°O), VIII Región Chile, Provincia del Neuquén, Argentina: Implicancias en la tectónica regional. Master's Thesis, Universidad de Concepción, 108 pp.

Melnick, D., Rosenau, M., Folguera, A., Echtler, H., 2006, Neogene tectonic evolution of the Neuquén Andes western flank (37–39°S). S.M. Kay, V.A. Ramos (eds), Evolution of an Andean margin: a tectonic and magmatic view from the Andes to the Neuquén Basin (35°–39°S lat), Geological Society of America Special Paper 407, 73–95.

Moreno, H., Lahsen, A., 1986. El volcán Callaqui: ejemplo de volcanismo fisural en los Andes del Sur. Revista de la Asociación Geológica Argentina 42, 1–8.

Muñoz, J., Stern, C., 1988. The Quaternary volcanic belt of the southern continental margin of South America: transverse structural and

petrochemical variations across the segment between 38° and 39°S. Journal of South American Earth Science 1, 147–161.

Muñoz, J., Stern, C., 1989. Alkaline magmatism within the segment 38°–39°S of the Plio–Quaternary volcanic belt of the Southern South American continental margin. Journal of Geophysical Research 94, 4545–4560.

Nakamura, K., 1977. Volcanoes as possible indicators of tectonic stress orientation: principles and proposal. Journal of Volcanology and Geothermal Research 2, 1–16.

Naranjo, J.A., Polanco, E., 2004. The 2000 AD eruption of Copahue Volcano, Southern Andes. Revista Geológica de Chile 31, 279–292.

Nelson, M.R., Forsythe, R., Arit, I., 1994. Ridge collision tectonics in terrane development. Journal of South American Earth Sciences 7, 271–278.

Niemeyer, H., Muñoz, J., 1983. Hoja Laguna de La Laja, Región del Bío-Bío, scale 1:250.000, Servicio Nacional de Geología y Minería.

Pasquarè, G., Garduno, V.H., Tibaldi, A., Ferrari, M., 1988. Stress pattern evolution in the Central Sector of the Mexican Volcanic Belt. Tectonophysics 146, 352–364.

Pasquarè, F.A., Tibaldi, A., 2003. Do transcurrent faults guide volcano growth? The case of NW Bicol Volcanic Arc, Luzon, Philippines. Terra Nova 15, 204–212.

Pesce, A., 1989. Evolución volcano-tectónica del complejo efusivo Copahue–Caviahue y su modelo geotérmico preliminar. Revista de la Asociación Geológica Argentina 44, 307–327.

Polanco, E., Naranjo, J.A., Young, S., Moreno, H., 2000. Volcanismo Explosivo Holoceno en la cuenca del alto Bío-Bío, Andes del Sur (37°45′–38°30′S). IX Congreso Geológico Chileno (Puerto Varas), Abstracts 2, 59–61.

Potent, S., Reuther, C.D., 2001. Neogene Deformationsprozesse im aktiven magmatischen Bogen Südzentralchiles zwischen 37° und 39°S. Mitteilungen Geologisch-Paläontologisches Institut Universität Hamburg 85, 1–22.

Potent, S., 2003. Kinematik und Dynamik neogener Deformationsprozesse des südzentralchilenischen Subduktionssystems, nördlichste Patagonische Anden (37°–40°S). Ph.D Thesis, Universität Hamburg, 169 pp.

Pubellier, M., Garcia, F., Loevenbruck, A., Chorowicz, J., 2000. Recent deformation at the junction between the North Luzon block and the Central Philippines from ERS-1 Images. The Island Arc 9, 598–610.

Radic, J.P., Rojas, L., Carpinelli, A., Zurita, E., 2002. Evolución Tectónica de la cuenca Terciaria de Cura-Mallín Región Cordillerana Chileno Argentina (36°30′–39°00′S). XIV Congreso Geológico Chileno (Calafate), electronic files.

Ramos, V.A., 1977. Estructura de la Cuenca Neuquina. VII Congreso Geológico Argentino (Neuquén), Abstracts, 98–118.

Ramos, V.A., Folguera, A., 1999. The Andes of Neuquén (36°–38°S): Evidence of Cenozoic transtension along the arc. IV Andean Geodynamic Symposium (Göttingen), Extended Abstracts, 606–609.

Reinecker, J., Heidbach, O., Tingay, M., Connolly, P., Müller, B., 2004. The 2004 release of the World Stress Map (available online at www.world-stress-map.org).

Rosenau, M., 2004. Tectonics of the southern Andean intra-arc zone (38°–42°S). Ph.D. Thesis, Freie Universität Berlin, 159 pp.

Rosenau, M., Melnick, D., Echtler, H., 2006. Kinematic constraints on intra-arc shear and strain partitioning in the Southern Andes between 38°S and 42°S latitude, Tectonics 25, TC4013.

Scheuber, E., Reutter, K., 1992. Magmatic arc tectonics in the Central Andes between 21° and 25°S. Tectonophysics 205, 127–140.

SERNAGEOMIN, 2002. Mapa Geológico de Chile, scale 1:1,000,000, Servicio Nacional de Geología y Minería.

Sieh, K., Natawidjaja, D., 2000. Neotectonics of the Sumatran fault, Indonesia. Journal of Geophysical Research 105, 28,295–28,326.

Somoza, R., 1998. Updated Nazca (Farallon)-South American relative motions during the last 40 My: implications for mountain bulding in the Andes. Journal of South American Earth Sciences 11, 211–215.

Suárez, M., Emparán, G., 1997. Hoja Curacautín, Regiones de la Araucanía y del Bío-Bío, scale 1:250,000, Servicio Nacional de Geología y Minería.

Tibaldi, A., 1992. The role of transcurrent intra-arc tectonics in the configuration of a volcanic arc. Terra Nova 4, 567–577.

Tibaldi, A., 1995. Morphology of pyroclastic cones and tectonics. Journal of Geophysical Research 100, 24,521–24,535.

Tikoff, B., Teyssier, C., 1994. Strain modeling of displacement-field partitioning in transpressional orogens. Journal of Structural Geology 16, 1575–1588.

Varekamp, J., Ouimette, A., Herman, S., Bermúdez, A., Delpino, D., 2001. Hydrothermal element fluxes from Copahue, Argentina: a "beehive" volcano in turmoil. Geology 29, 1059–1062.

Vergara, M., Muñoz, J., 1982. La Formación Cola de Zorro en la alta cordillera Andina Chilena (36°–39° Lat. S), sus características petrográficas y petrológicas: una revisión. Revista Geológica de Chile 17, 31–46.